ARMY RESEARCH LABORATORY

Finite Deformations and Internal Forces in Elastic-Plastic Crystals: Interpretations From Nonlinear Elasticity and Anharmonic Lattice Statics

by J. D. Clayton and D. J. Bammann

ARL-RP-274 **September 2009**

A reprint from *Journal of Engineering Materials and Technology,* Vol. 131, pp. 041201-1–041201-15, October 2009.

NOTICES

Disclaimers

The findings in this report are not to be construed as an official Department of the Army position unless so designated by other authorized documents.

Citation of manufacturer's or trade names does not constitute an official endorsement or approval of the use thereof.

Destroy this report when it is no longer needed. Do not return it to the originator.

Army Research Laboratory
Aberdeen Proving Ground, MD 21005-5066

ARL-RP-274 **September 2009**

Finite Deformations and Internal Forces in Elastic-Plastic Crystals: Interpretations From Nonlinear Elasticity and Anharmonic Lattice Statics

J. D. Clayton
Weapons and Materials Research Directorate, ARL

D. J Bammann
Mississippi State University

A reprint from *Journal of Engineering Materials and Technology,* Vol. 131, pp. 041201-1–041201-15, October 2009.

REPORT DOCUMENTATION PAGE

Form Approved
OMB No. 0704-0188

1. REPORT DATE *(DD-MM-YYYY)*	2. REPORT TYPE	3. DATES COVERED (From - To)
September 2009	Reprint	October 2009

4. TITLE AND SUBTITLE
Finite Deformations and Internal Forces in Elastic-Plastic Crystals: Interpretations From Nonlinear Elasticity and Anharmonic Lattice Statics

5a. CONTRACT NUMBER

5b. GRANT NUMBER

5c. PROGRAM ELEMENT NUMBER

6. AUTHOR(S)
J. D. Clayton and D. J. Bammann*

5d. PROJECT NUMBER

5e. TASK NUMBER

5f. WORK UNIT NUMBER

7. PERFORMING ORGANIZATION NAME(S) AND ADDRESS(ES)
U.S. Army Research Laboratory
ATTN: RDRL-WMT-D
Aberdeen Proving Ground, MD 21005-5066

8. PERFORMING ORGANIZATION REPORT NUMBER
ARL-RP-274

9. SPONSORING/MONITORING AGENCY NAME(S) AND ADDRESS(ES)

10. SPONSOR/MONITOR'S ACRONYM(S)

11. SPONSOR/MONITOR'S REPORT NUMBER(S)

12. DISTRIBUTION/AVAILABILITY STATEMENT
Approved for public release; distribution is unlimited.

13. SUPPLEMENTARY NOTES
A reprint from *Journal of Engineering Materials and Technology,* Vol. 131, pp. 041201-1–041201-15, October 2009.
*Center for Advanced Vehicular Systems, Mississippi State University, Starkville, MS 39762

14. ABSTRACT
Large deformation kinematics and internal forces arising from defects in crystalline solids are addressed by a nonlinear kinematic description and multiscale averaging concepts. An element of crystalline material with spatially uniform properties and containing defects such as dislocation lines and loops is considered. The average deformation gradient for this element is decomposed multiplicatively into terms accounting for effects of dislocation flux, recoverable elastic stretch and rotation, and residual elastic deformation associated with self-equilibrating internal forces induced by defects. Two methods are considered for quantifying average residual elastic deformation: continuum elasticity and discrete lattice statics. Average residual elastic strains and corresponding average residual elastic volume changes are negligible in the context of linear elasticity or harmonic force potentials but are not necessarily inconsequential in the more general case of nonlinear elasticity or anharmonic interactions.

15. SUBJECT TERMS
elasticity, plasticity, dislocations, lattice statics, molecular dynamics, multiscale modeling, nonlinear elasticity

16. SECURITY CLASSIFICATION OF:			17. LIMITATION OF ABSTRACT	18. NUMBER OF PAGES	19a. NAME OF RESPONSIBLE PERSON
a. REPORT	b. ABSTRACT	c. THIS PAGE			John D. Clayton
Unclassified	Unclassified	Unclassified	UU	22	19b. TELEPHONE NUMBER (*Include area code*) 410-278-6146

Finite Deformations and Internal Forces in Elastic-Plastic Crystals: Interpretations From Nonlinear Elasticity and Anharmonic Lattice Statics

J. D. Clayton
Mem. ASME
Impact Physics,
US Army Research Laboratory,
Aberdeen Proving Ground, MD 21005
e-mail: jclayton@arl.army.mil

D. J. Bammann
Fellow ASME
Center for Advanced Vehicular Systems,
Mississippi State University,
Starkville, MS 39762
e-mail: bammann@cavs.msstate.edu

Large deformation kinematics and internal forces arising from defects in crystalline solids are addressed by a nonlinear kinematic description and multiscale averaging concepts. An element of crystalline material with spatially uniform properties and containing defects such as dislocation lines and loops is considered. The average deformation gradient for this element is decomposed multiplicatively into terms accounting for effects of dislocation flux, recoverable elastic stretch and rotation, and residual elastic deformation associated with self-equilibrating internal forces induced by defects. Two methods are considered for quantifying average residual elastic deformation: continuum elasticity and discrete lattice statics. Average residual elastic strains and corresponding average residual elastic volume changes are negligible in the context of linear elasticity or harmonic force potentials but are not necessarily inconsequential in the more general case of nonlinear elasticity or anharmonic interactions. [DOI: 10.1115/1.3183773]

Keywords: nonlinear elasticity, plasticity, lattice statics, dislocations, multiscale modeling

1 Introduction

By typical definition, plastic deformation in crystalline solids takes place by the motion or flux of distributions of dislocations [1,2]. An element of material through which a net flux of dislocations has passed exhibits a permanent (plastic) shape change [3]. The dislocation lines within the element, i.e., displacement discontinuities across the slip plane in the context of Volterra defects in elastic continua, may also contribute to this plastic deformation [4–7]. However, plastic deformation in this context does not explicitly account for the additional change in dimensions of the body due to residual elastic deformation associated with local stress fields (i.e., eigenstresses [7]) induced by defects. For example, dislocation glide preserves the volume of the crystal, and tangential displacement (i.e., slip) discontinuities do not alter the volume occupied by the material. Yet ample evidence suggests that dislocation lines affect the volume of crystals [8–11]. Stored energies associated with elastic fields of defects are important because they affect recrystallization [9,12] and the fraction of stress power converted to temperature rise at high deformation rates [13] that can lead to strain softening and shear localization in metals during dynamic failure events. Large numbers of dislocations, twins, and stacking faults can be generated during shock loading [14], and presumably the corresponding volume changes, shape changes, and stored energies associated with local stress fields of these defects affect the observed response (e.g., pressure-volume or stress-strain profiles) under such conditions [15].

Defects of interest in the present work are those that can be described in a continuum sense by closed displacement discontinuities tangential to an internal surface (i.e., crystallographic plane) in a volume element of material. These include gliding straight or curved dislocations lines, dislocation loops, as well as partial dislocations. Motion of dislocation defects through a region of the crystal results in plastic shape change as mentioned above but preserves the lattice spacing [3]; this requires cooperative motion of leading and trailing partials for the case of partial dislocations. Residual elastic stress fields from disclination lines and loops are also considered [6,16,17], though their contribution to the plastic shape change [18] is not addressed explicitly. Also not considered are voids, fractures, and point defects [19,20] that may have finite volume and affect the lattice differently. Dislocation climb is also not considered here, because it generally involves vacancy migration [21].

Modeling efforts directed toward large deformation kinematics of crystalline solids feature a long history. In the absence of defects, thermal or electromagnetic effects, or internal relative displacements among atoms of different sublattices, a deformation gradient $\mathbf{F}$ applied uniformly over an element of mechanically stressed material and the linear mapping $\mathbf{F}^{\mathbf{E}}$ of its interatomic bond vectors (i.e., primitive Bravais lattice vectors and basis vectors at each lattice point) coincide. This is typically called the Cauchy–Born hypothesis [22,23] and is written as $\mathbf{F}=\mathbf{F}^{\mathbf{E}}$. When plastic deformation takes place, the description is typically extended to $\mathbf{F}=\mathbf{F}^{\mathbf{E}}\mathbf{F}^{\mathbf{P}}$ [3,24,25], where $\mathbf{F}^{\mathbf{P}}$ accounts for the presence and motion of dislocations or other defects. The idea of a relaxed intermediate or natural configuration implicit in this multiplicative decomposition was introduced somewhat earlier [26]. Early studies of continuously distributed lattice defects considered self-stresses and residual elastic deformations resulting from defects [27–29]. In such instances the plastic deformation $\mathbf{F}^{\mathbf{P}}$ inducing discontinuities in the first place was often not considered explicitly, nor was elastic deformation $\mathbf{F}^{\mathbf{E}}$ associated with external loading, since the element of material containing defects was in a state of self-stress. Defect content associated with heterogeneous elastic

Contributed by the Materials Division of ASME for publication in the JOURNAL OF ENGINEERING MATERIALS AND TECHNOLOGY. Manuscript received January 14, 2009; final manuscript received March 30, 2009; published online August 27, 2009. Assoc. Editor: Hussein Zbib.

and inelastic deformations (i.e., tangent mappings in the multiplicative decomposition) can be described using tensor calculus and differential geometry [3,16,24,30–37].

In this work a three-term decomposition, $\mathbf{F}=\mathbf{F}^{\mathbf{E}}\mathbf{F}^{\mathbf{I}}\mathbf{F}^{\mathbf{P}}$, is assigned to describe the kinematics of a volume element of crystalline material containing lattice defects. For simplicity, isothermal conditions are assumed (e.g., no thermal expansion). Elastic tangent map $\mathbf{F}^{\mathbf{E}}$ used here is analogous to that of Born, Huang, and Ericksen [22,23,38]. Plastic tangent map $\mathbf{F}^{\mathbf{P}}$ results from cumulative effects of fluxes of dislocations [1,2,39] and slip discontinuities associated with defects within the element [4,5]. Intermediate term $\mathbf{F}^{\mathbf{I}}$ (or its stretch or rotational components) has been introduced in a number of works with various definitions [16,34–36,40–42]. Here $\mathbf{F}^{\mathbf{I}}$ represents the average residual elastic deformation of the element induced by local stress and strain fields of defects contained within, and corresponds to the volume average of residual elastic deformation in the context of defect field theories [27–29].

In Sec. 3, the externally unloaded volume element is treated as an elastic body with homogeneous elastic constants, in static equilibrium, and containing internal displacement discontinuities across which traction is continuous. The element is free of external traction but may support residual stresses. The self-equilibrium conditions result in an integral equation for $\mathbf{F}^{\mathbf{I}}$. For linear-elastic constitutive behavior, $\mathbf{F}^{\mathbf{I}}$ reduces to the unit tensor in rectangular Cartesian coordinates, but $\mathbf{F}^{\mathbf{I}}$ does not so reduce for nonlinear behavior. Following previous studies [29,43,44], volume changes resulting from the stored energy of defect lines are considered for cubic and isotropic crystals. A proportionality relationship between the line density of dislocations or disclinations per unit reference volume of the solid and this residual volume change is obtained. Analytical elasticity solutions for defect energies are considered along with experimental data [45] to confirm accuracy of the theory.

In Sec. 4, the externally unloaded volume element is identified as a set of discrete atoms in static equilibrium and free of external forces. According to this description, all interatomic forces vanish in a perfect lattice free of defects (e.g., no bond stretching), but nonzero forces may exist among atoms when they are arranged in an imperfect way (i.e., when defects are present). In this case, the self-equilibrium conditions are equivalent to vanishing of static components of the average virial stress for the set of atoms [38,46]. The potential energy is expanded about a perfect reference state, leading to expressions for stress and elastic stiffness tensors in terms of harmonic and anharmonic parts of the potential. When atomic interactions are harmonic, equilibrium demands that $\mathbf{F}^{\mathbf{I}}$ as defined here should reduce to the unit tensor, analogously to the linear-elastic continuum interpretation. However, in the more general scenario of anharmonic interactions [47–49] that may be physically significant in the vicinity of defect cores where large atomic displacements arise, the derivations suggest $\mathbf{F}^{\mathbf{I}}$ could be non-negligible.

A number of theoretical models have introduced a term akin to $\mathbf{F}^{\mathbf{I}}$ to represent elastic fields of crystal defects [16,34,35,41], though previous works did not always include precise mathematical definitions for $\mathbf{F}^{\mathbf{I}}$ or quantitative estimates of its magnitude in engineering materials. The present work gives exact definitions for $\mathbf{F}^{\mathbf{I}}$ using anisotropic nonlinear continuum elasticity (Sec. 3) and discrete lattice statics (Sec. 4). Also, the present work demonstrates how residual elastic volume changes ($\approx \det \mathbf{F}^{\mathbf{I}}$) can be estimated for defect lines, extending earlier analysis [43] to address geometric nonlinearity. Previous authors [8,10,43] did not emphasize possible shape changes associated with $\mathbf{F}^{\mathbf{I}}$ (though Toupin and Rivlin [44] mentioned shape changes briefly) nor did they attempt to place their derivations in the context of multiplicative elastoplasticity as demonstrated in the present work. The new atomic-scale definition of $\mathbf{F}^{\mathbf{I}}$ in Sec. 4 may prove useful in the context of multiscale computations of nonlinear elastic and plastic properties of crystals [50,51] and offers a more accurate treatment of defect cores than classical continuum elasticity.

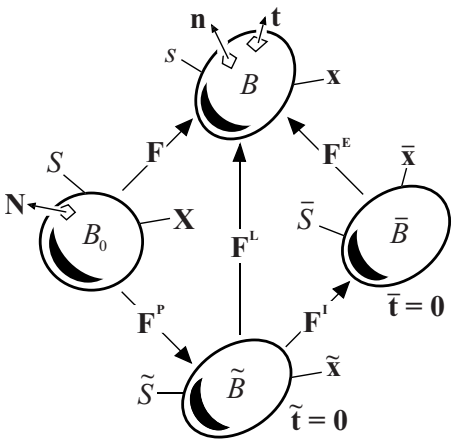

Fig. 1 Configurations, surface coordinates, traction vectors, and tangent mappings

The following notation is used. Scalars and individual components of vectors and tensors are written in italics, while vectors and tensors are written in bold. Einstein's summation convention applies for repeated indices. The • symbol denotes the scalar product of vectors ($\mathbf{a}\cdot\mathbf{b}=a^a b_a=a^1b_1+a^2b_2+a^3b_3$), while $\otimes$ indicates the outer product ($(\mathbf{a}\otimes\mathbf{b})^{ab}=a^a b^b$). Juxtaposition of second-rank tensors implies summation over one set of adjacent indices ($(\mathbf{AB})^a_{.c}=A^{ab}B_{bc}$). Indices in parentheses are symmetric ($2A_{(ab)}=A_{ab}+A_{ba}$). Superposed -1 denotes inversion. Subscripted commas denote partial differentiation.

2 Kinematics of Deformation

Consider a volume element of a crystal containing lattice defects. This element is of a size larger than the atomic spacing but may be of smaller dimensions than the entire crystal. Static and isothermal conditions are assumed. Deformation of the element is described by mappings between tangent spaces of configurations, as shown in Fig. 1. Reference configuration B_0 is a perfect lattice. Position vector $\mathbf{R}_{\langle m\rangle}$ of atom m (e.g., the equilibrium position of its nucleus) relative to the origin of a Cartesian coordinate system in an infinite lattice in the reference configuration is given by the periodicity relations [22,23]

$$\mathbf{R}_{\langle m\rangle}=\mathbf{z}_{\langle m\rangle}+\sum_{k=1}^{3} i_{\langle m\rangle k}\mathbf{A}^k \tag{1}$$

where $i_{\langle m\rangle k}$ are integers and $\mathbf{A}^k$ are the primitive Bravais lattice vectors. Basis vector $\mathbf{z}_{\langle m\rangle}$ denotes the reference position of atom m of the basis at each point on the Bravais lattice relative to the origin of the corresponding primitive unit cell. For a monatomic basis, $\mathbf{z}_{\langle m\rangle}=\mathbf{0}$.

2.1 Plastic Deformation. Intermediate configuration $\tilde{B}$ in Fig. 1 differs from B_0 due to influences of cumulative motion of lattice defects and perturbations of atomic positions resulting from these defects. Configuration $\tilde{B}$ is by definition free of external traction ($\tilde{\mathbf{t}}=\mathbf{0}$) and free of internal stresses. For a crystal containing a single dislocation, a singular plastic deformation map can be defined as [4,5]

$$\mathbf{F}^{\mathbf{P}}=\mathbf{1}+\mathbf{b}\otimes\mathbf{M}\delta(\mathbf{X}\cdot\mathbf{M})\chi \tag{2}$$

where $\mathbf{1}$ is the unit tensor, $\mathbf{b}$ is the Burgers vector, $\mathbf{M}$ is the normal to the slip surface in the reference configuration, δ is the Dirac delta function, and χ is the characteristic function that is unity at

reference coordinates $\mathbf{X}$ on slipped surface Σ and zero elsewhere. The Cartesian coordinate system for $\mathbf{X}$ is chosen with its origin in the slip plane. A dislocation density tensor corresponding to Eq. (2) is [4]

$$\boldsymbol{\alpha} = \mathbf{b} \otimes \boldsymbol{\xi}_0 \delta(L) \tag{3}$$

where $\boldsymbol{\xi}_0$ is the unit tangent to the dislocation line L in the reference configuration. From Eqs. (2) and (3),

$$\mathbf{b} = -\int_{\mathbf{X}^+}^{\mathbf{X}^-} \mathbf{F}^{\mathbf{P}} d\mathbf{X} = \int_A \boldsymbol{\alpha} \mathbf{N} dA \tag{4}$$

where the line integral in the first of Eq. (4) takes place across coordinates above ($\mathbf{X}^+$) and below ($\mathbf{X}^-$) the slipped surface, and integration in the second of Eq. (4) proceeds over oriented area A with unit normal $\mathbf{N}$ such that $\boldsymbol{\xi}_0 \cdot \mathbf{N} = 1$ at the intersection of L and A. If defects are introduced sequentially, a logical nonsingular extension of Eq. (2) for a volume element containing multiple dislocation lines is

$$\mathbf{F}^{\mathbf{P}} = \prod_{m=1}^{n} \left(\mathbf{1} + V^{-1} \int \mathbf{b} \otimes \mathbf{M} \delta(\Sigma) dV \right) = \prod_{m=1}^{n} (\mathbf{1} + V^{-1} \mathbf{b} \otimes \mathbf{M} \Sigma) \tag{5}$$

where the product is taken over n dislocations, each with a possibly different Burgers vector $\mathbf{b}$ and constant normal vector $\mathbf{M}$ to an assumed flat slipped surface of reference area Σ. The volume of the element in the reference configuration is denoted by V. Note that Eq. (5) depends on the order in which each dislocation is introduced. Since $\mathbf{b} \perp \mathbf{M}$, Eq. (5) consists of a product of simple shears and volume is conserved, i.e., $J^P = \det \mathbf{F}^{\mathbf{P}} = 1$. For a collection of j straight stationary dislocation line populations of density $\rho^i = \lim_{V \to 0} (L^i / V)$, Burgers vector $\mathbf{b}^i$, unit tangent $\boldsymbol{\xi}_0^i$, and plane normal $\mathbf{M}^i$, the dislocation density in Eq. (3) and Burgers integral in Eq. (4) can be extended as

$$\boldsymbol{\alpha} = V^{-1} \int_L \mathbf{b} \otimes \boldsymbol{\xi}_0 dL = \sum_{i=1}^{j} \rho^i \mathbf{b}^i \otimes \boldsymbol{\xi}_0^i \tag{6}$$

$$\mathbf{B} = \int_A \boldsymbol{\alpha} \mathbf{N} dA = \int_A \sum_{i=1}^{j} \rho^i \mathbf{b}^i (\boldsymbol{\xi}_0^i \cdot \mathbf{N} dA) \tag{7}$$

with $\mathbf{B}$ the summed projection of all local Burgers vectors $\mathbf{b}$ of dislocation lines passing through area A. The line integration in Eq. (6) proceeds over all dislocations of total length L. The second of Eq. (6) pertains to j dislocation populations with the same tangent line and local Burgers vector for each value of i.

A more general definition of average plastic deformation of a volume element accounts for the history of generation and motion of defects within it, in which case $\mathbf{F}^{\mathbf{P}}$ is defined as the solution of

$$\dot{\mathbf{F}}^{\mathbf{P}} = \mathbf{L}^{\mathbf{P}} \mathbf{F}^{\mathbf{P}}, \quad \mathbf{F}^{\mathbf{P}}|_{t=0} = \mathbf{1} \tag{8}$$

Average plastic velocity gradient $\mathbf{L}^{\mathbf{P}}$ is dictated by the flux $\tilde{\boldsymbol{\varsigma}}$ of mobile dislocations [2,17,39,52]:

$$L_{.\beta}^{P\alpha} = \tilde{\varsigma}^{\alpha\chi\delta} \tilde{\varepsilon}_{\chi\delta\beta}, \quad \tilde{\varsigma}^{\alpha\chi\delta} = V^{-1} \int_L b^{i\alpha} \tilde{\xi}^{i\chi} \tilde{v}^{i\delta} dL = \sum_{i=1}^{j} \rho^i b^{i\alpha} \tilde{\xi}^{i\chi} \tilde{v}^{i\delta} \tag{9}$$

where $\tilde{\boldsymbol{\varepsilon}}$ is the permutation tensor, and $\tilde{\boldsymbol{\xi}}^i$ and $\tilde{\mathbf{v}}^i$ are, respectively, the uniform tangent line and velocity of every dislocation in population i. All vector and tensor indices written in Greek font in Eq. (9) are subject to the Einstein summation convention and are referred to configuration $\tilde{B}$. Since dislocation segments have perpendicular velocities and tangent lines, $\dot{J}^P = J^P \operatorname{tr} \mathbf{L}^{\mathbf{P}} = 0$ and $J^P = 1$. Relation (9) applies for straight dislocations; similar expressions can be formulated for dislocation loops [4]. Introducing the notation $\tilde{\boldsymbol{\xi}}^i \times \tilde{\mathbf{v}}^i = \tilde{\mathbf{m}}^i v^i$, $v^i = |\tilde{\mathbf{v}}^i|$, $\mathbf{b}^i = b^i \tilde{\mathbf{s}}^i$, and $b^i = |\mathbf{b}^i|$, where $\tilde{\mathbf{m}}^i$ is the unit normal to the slip plane and $\tilde{\mathbf{s}}^i$ is a unit vector in the direction of slip, Eq. (9) reduces to [5,53]

$$\mathbf{L}^{\mathbf{P}} = \sum_i \rho^i b^i v^i \tilde{\mathbf{s}}^i \otimes \tilde{\mathbf{m}}^i = \sum_i \dot{\gamma}^i \tilde{\mathbf{s}}^i \otimes \tilde{\mathbf{m}}^i \tag{10}$$

Rate equation $\dot{\gamma}^i = \rho^i b^i v^i$ [1] implies that only mobile dislocations contribute to Eq. (10). Since $\tilde{\mathbf{s}}^i \perp \tilde{\mathbf{m}}^i$, $\dot{J}^P = J^P \operatorname{tr} \mathbf{L}^{\mathbf{P}} = 0$ and $J^P = 1$. In summary, according to definitions in the context of single dislocations (2) and (5), dislocation flux (9), or crystal plasticity theory (10), plastic deformation is isochoric.

2.2 Lattice Deformations. Let $\mathbf{F}^{\mathbf{E}}$ denote the tangent map to externally stressed spatial configuration B (generally with $\mathbf{t} \neq \mathbf{0}$ in Fig. 1) from self-equilibrated configuration $\bar{B}$ ($\bar{\mathbf{t}} = \mathbf{0}$ in Fig. 1). Let $\bar{\mathbf{a}}^k$ denote the primitive Bravais lattice vectors of Eq. (1) mapped to $\bar{B}$:

$$\bar{\mathbf{a}}^k = \mathbf{F}^{\mathbf{I}} \tilde{\mathbf{1}} \mathbf{A}^k \tag{11}$$

with $\tilde{\mathbf{1}}$ the shifter between coordinate frames in B_0 and $\tilde{B}$. When coincident coordinate systems are used in these two configurations, $\tilde{\mathbf{1}} = \mathbf{1}$. Note that lattice vectors are not affected by $\mathbf{F}^{\mathbf{P}}$, in accordance with continuous dislocation theory [3,34] and crystal plasticity theory [53]. Lattice vectors deform from $\bar{B}$ to B according to

$$\mathbf{a}^k = \mathbf{F}^{\mathbf{E}} \bar{\mathbf{a}}^k = \mathbf{F}^{\mathbf{L}} \tilde{\mathbf{1}} \mathbf{A}^k \tag{12}$$

where the total lattice deformation for the volume element is $\mathbf{F}^{\mathbf{L}} = \mathbf{F}^{\mathbf{E}} \mathbf{F}^{\mathbf{I}}$. Under a homogeneous deformation, basis vectors $\mathbf{z}_{\langle m \rangle}$ in Eq. (1) deform similarly to the primitive Bravais lattice vectors $\mathbf{A}^k$ in Eq. (12), though the final position of atom m may also change by an additional translation relative to its neighbors [22]. This translation may be due, for example, to polarization of a dielectric crystal in an applied electric field or inner displacements among sublattices in a noncentrosymmetric polyatomic crystal [54]. Relations (11) and (12) generalize the Cauchy–Born hypothesis [22,23], distinguishing the effects of recoverable ($\mathbf{F}^{\mathbf{E}}$) and residual ($\mathbf{F}^{\mathbf{I}}$) deformations on the lattice, and reduce to the prescription of Ericksen [23] when the effects of defects are absent in $\bar{B}$, such that $\mathbf{F}^{\mathbf{I}} = \mathbf{1}$. Rigid body rotations of the element are included in the rotational part of the polar decomposition of $\mathbf{F}^{\mathbf{L}}$, denoted by $\mathbf{R}^{\mathbf{L}}$. Reference Bravais lattice vectors $\mathbf{A}^k$ are uniform in a perfect homogeneous lattice. However, when defects are contained within the volume, deformed primitive lattice vectors $\mathbf{a}^k$ and $\bar{\mathbf{a}}^k$ represent suitable averages of local lattice vectors $\mathbf{a}'^k$ and $\bar{\mathbf{a}}'^k$ that may not be spatially constant:

$$\mathbf{a}^k = V^{-1} \int_V \mathbf{a}'^k dV, \quad \bar{\mathbf{a}}^k = V^{-1} \int_V \bar{\mathbf{a}}'^k dV \tag{13}$$

Configuration $\bar{B}$ can be obtained from the spatial configuration by cutting the volume element out of the stressed body thereby relieving the external traction, relaxing any possible internal viscous and inertial forces, and then rotating this element by $\mathbf{R}^{\mathbf{E}-1}$.

2.3 Total Deformation. Total deformation gradient $\mathbf{F}$ for the volume element is defined by the surface integral [55,56]

$$\mathbf{F} = V^{-1} \int_S \mathbf{x} \otimes \mathbf{N} dS \tag{14}$$

where $\mathbf{x}$ are spatial coordinates of the deformed image of reference surface S enclosing the volume element with unit outward reference normal $\mathbf{N}$, as shown in Fig. 1. The element may contain

discontinuities in internal displacement and gradients of displacement; when discontinuities are absent and after Gauss's theorem is applied, Eq. (14) reduces to $F^a_{\cdot A}=V^{-1}\int x^a_{,A}dV$, where $x^a=x^a(X^A,t)$ is now smooth within V. Assume that $\mathbf{F}$ is imposed on an element of material via Eq. (14), and that decomposition

$$\mathbf{F}=\mathbf{F^E}\mathbf{F^I}\mathbf{F^P}=\mathbf{F^L}\mathbf{F^P} \tag{15}$$

applies, as implied by Fig. 1. Plastic deformation $\mathbf{F^P}$ is known from integration of Eq. (8) with Eq. (9) or Eq. (10), presuming kinetic laws are available for the dislocation flux in Eq. (9) or the slip rates on each slip system in Eq. (10). Under isothermal conditions, the crystal responds to applied loading elastically such that

$$\overline{\mathbf{\Sigma}}=\overline{\mathbf{\Sigma}}(\mathbf{U^E})\leftrightarrow\mathbf{U^E}=\mathbf{U^E}(\overline{\mathbf{\Sigma}}) \tag{16}$$

where stretch $\mathbf{U^E}=\mathbf{R^{E-1}}\mathbf{F^E}=(\mathbf{F^{E}}^T\mathbf{F^E})^{1/2}$ is an invertible function of conjugate stress measure $\overline{\mathbf{\Sigma}}$ that vanishes when traction $\mathbf{t}=\mathbf{0}$ along deformed surface S of the element in Fig. 1. The particular form of Eq. (16) will depend on the orientation of the lattice in $\overline{B}$ because of anisotropy. Henceforth, it is assumed that

$$\mathbf{F^L}=\mathbf{R^E}\mathbf{U^E}\mathbf{F^I}=\mathbf{R^L}\mathbf{U^E}\mathbf{U^I},\quad \mathbf{F^I}=\mathbf{U^I} \tag{17}$$

meaning $\mathbf{F^I}$ is a stretch (symmetric with six independent entries in covariant Cartesian coordinates) and all lattice rotation is embedded in $\mathbf{R^E}$. The objective of Secs. 3 and 4 of the present paper is suggestion of approaches to obtain $\mathbf{F^I}$. Then if $\mathbf{F^P}$ is also known at a particular instant, $\mathbf{F^E}=\mathbf{F}\mathbf{F^{P-1}}\mathbf{F^{I-1}}$ can be found from Eq. (15) and the average external stress supported by the element can be updated according to constitutive relation (16).

3 Nonlinear Elastic Approach

The dimensional changes of a nonlinear elastic body in a state of self-stress, i.e., a self-equilibrated body with internal residual stresses but no traction applied to its external boundaries, are derived in Secs. 3.1–3.3. The body may contain one or more internal surfaces across which traction is continuous but tangential displacements are not. The treatment is specialized in Sec. 3.4 to address volume changes in cubic crystals and then isotropic materials. Formulas for volume changes attributed to local elastic stress fields of line defects are derived in the isotropic approximation in Sec. 3.5. Derivations and discussion in Secs. 3.1–3.5 consolidate and extend prior work of a number of authors [8,29,43,44]. Additional analysis and examples follow in Secs. 3.6 and 3.7.

3.1 Average Stress Measures. The local balance of linear momentum is written in rectangular Cartesian coordinates as

$$P^{aA}_{\cdot\cdot,A}+\overline{B^a}=\rho_0 A^a \tag{18}$$

with $\overline{B^a}$ the body force per unit reference volume, ρ_0 the reference mass density, and A^a the material acceleration. In reference coordinates X^A, Eq. (18) provides the relation

$$(X^A P^{aB})_{,B}=P^{aA}+(\rho_0 A^a-\overline{B^a})X^A \tag{19}$$

Consider a body of reference volume V with external surface S. The body may contain closed internal surfaces across which displacement from the reference state (e.g., a perfect lattice) and stress fields are discontinuous, but traction per unit reference area t_0^a across internal surfaces is continuous:

$$t_0^{+a}-t_0^{-a}=(P^{+aA}-P^{-aA})M_A=0\quad(\text{on }\Sigma) \tag{20}$$

where + and − denote the limiting values of a quantity near the surface as the surface is approached from either side, M_A is a normal vector to an internal surface, and Σ denotes the union of such internal surfaces. The source of the displacement discontinuities across Σ is arbitrary in Eq. (20); however, for the particular case of dislocation(s) within V, jump(s) in displacement across the slip planes comprising Σ are attributed to the Burgers vector(s) introduced in Eqs. (2) and (5). Integrating Eq. (19) over V and applying the divergence theorem,

$$\int_V P^{aA}dV=\int_S X^A P^{aB}N_B dS+\int_\Sigma X^A(P^{+aB}-P^{-aB})M_B d\Sigma+\int_V X^A(\overline{B^a}-\rho_0 A^a)dV \tag{21}$$

where N_B are components of the external normal to V of Eq. (14). Applying Eq. (20), and considering now a body in static equilibrium,

$$\int_V P^{aA}dV=\int_S X^A P^{aB}N_B dS=\int_S t_0^a X^A dS \tag{22}$$

For a self-equilibrated body, $t_0^a=0$ by definition, and Eq. (22) reduces to

$$V^{-1}\int_V P^{aA}dV=0 \tag{23}$$

meaning that the integrated or volume-averaged first Piola–Kirchhoff stress vanishes over the reference volume. Now consider the balance of linear momentum in the spatial configuration,

$$\sigma^{ab}_{\cdot\cdot,b}+\overline{b^a}=\rho a^a \tag{24}$$

with $\sigma^{ab}=\det(X^A_{\cdot,a})x^a_{\cdot,A}P^{bA}$, $\overline{b^a}$ the body force per unit current volume, $\rho=\rho_0\det(X^A_{\cdot,a})$, and a^a the spatial acceleration. Spatial analogs of Eqs. (19)–(21) are

$$(x^b\sigma^{ac})_{,c}=\sigma^{ab}+(\rho a^a-\overline{b^a})x^b \tag{25}$$

$$t^{+a}-t^{-a}=(\sigma^{+ab}-\sigma^{-ab})m_b=0\quad(\text{on }\sigma) \tag{26}$$

$$\int_v \sigma^{ab}dv=\int_s x^b\sigma^{ac}n_c ds+\int_\sigma x^b(\sigma^{+ac}-\sigma^{-ac})m_c d\sigma+\int_v x^b(\overline{b^a}-\rho a^a)dv \tag{27}$$

with x^a the spatial coordinates, t^a the traction per unit current area, σ the union of closed internal boundaries, m_a the unit normal to internal surfaces, n_a the unit normal to external surface S (Fig. 1), and v the current volume of the body enclosed by s. For a body in static equilibrium,

$$\int_v \sigma^{ab}dv=\int_s x^b\sigma^{ac}n_c ds=\int_s t^a x^b ds \tag{28}$$

and for a self-equilibrated body,

$$v^{-1}\int_v \sigma^{ab}dv=0 \tag{29}$$

i.e., the average Cauchy stress vanishes over the spatial volume of the body.

3.2 Hyperelasticity. In the present treatment, the constitutive response of the material is assumed hyperelastic, with effects of temperature change neglected. Let $\Psi_0=\Psi_0(E_{AB})$ denote the strain energy per unit reference volume of the solid, with the symmetric Lagrangian strain

$$E_{AB} = \tfrac{1}{2}(x^a_{.,A}\delta_{ab}x^b_{.,B} - \delta_{AB}) = \delta^a_{.A}u_{(a,B)} + \tfrac{1}{2}u_{c,A}u^c_{.,B} \tag{30}$$

where coincident Cartesian coordinates are assigned in reference and spatial configurations and $u^a = x^a - \delta^a_{.A}X^A$ is the local displacement. Let

$$\Psi_0 = \frac{1}{2!}\mathbb{C}^{ABCD}E_{AB}E_{CD} + \frac{1}{3!}\mathbb{C}^{ABCDEF}E_{AB}E_{CD}E_{EF} + \ldots \tag{31}$$

where second- and third-order elastic constants are evaluated from a series expansion of the energy density about the unstrained state of the crystal as, respectively,

$$\mathbb{C}^{ABCD} = \left.\frac{\partial^2\Psi_0}{\partial E_{AB}\,\partial E_{CD}}\right|_{\mathbf{E}=\mathbf{0}}, \quad \mathbb{C}^{ABCDEF} = \left.\frac{\partial^3\Psi_0}{\partial E_{AB}\,\partial E_{CD}\,\partial E_{EF}}\right|_{\mathbf{E}=\mathbf{0}} \tag{32}$$

Usual symmetries of elastic moduli are evident from Eqs. (31) and (32). The local first Piola–Kirchhoff stress following from Eq. (31) is

$$P^{aA} = \frac{\partial\Psi_0}{\partial x_{a,A}} = \frac{\partial\Psi_0}{\partial u_{a,A}} = x^a_{.,B}\frac{\partial\Psi_0}{\partial E_{AB}} = x^a_{.,B}\left(\mathbb{C}^{ABCD}E_{CD} + \frac{1}{2}\mathbb{C}^{ABCDEF}E_{CD}E_{EF} + \ldots\right) \tag{33}$$

Using symmetry properties of the moduli from Eq. (32) and neglecting terms of degree higher than 3 in the displacement gradients $u_{A,B} = \delta^b_{.A}u_{b,B}$, Eq. (31) can be written as [44]

$$\Psi_0 = \tfrac{1}{2}\mathbb{C}^{ABCD}u_{A,B}u_{C,D} + \tfrac{1}{2}\mathbb{C}^{ABCD}u_{A,B}u_{E,C}u^E_{.,D} + \tfrac{1}{6}\mathbb{C}^{ABCDEF}u_{A,B}u_{C,D}u_{E,F} \tag{34}$$

3.3 Average Residual Elastic Deformation. Consider externally unloaded configuration of the volume element labeled $\overline{B}$ in Fig. 1. This configuration corresponds to the deformed but self-equilibrated body obeying Eqs. (23) and (29). The reference configuration with internal displacement discontinuities described in Eqs. (18)–(34) now corresponds to stress-free intermediate configuration $\widetilde{B}$ of Fig. 1. As discussed by De Wit [6], displacement discontinuities attributed to Volterra dislocations lead to discontinuities in local plastic strain and rotation fields across slip planes or internal surfaces Σ within the volume, which owing to the isochoric nature of slip is preserved according to $\widetilde{V} = J^P V = V$. Such effects are quantified according to Eqs. (2)–(10), wherein discontinuities are introduced by the plastic deformation $\mathbf{F^P}$ between configurations B_0 and $\widetilde{B}$. Residual deformations are introduced within the element from the mapping between configurations $\widetilde{B}$ and $\overline{B}$. Locally, such deformations are treated as continuous, differentiable, and elastic between $\widetilde{B}$ and $\overline{B}$, with corresponding local displacement gradient and Lagrangian strain fields (i.e., eigenstrains) within the element denoted by $u_{A,B}$ and E_{AB}, respectively. This implies that the body has been resealed after the introduction and passage of defects in agreement with the definition of a Volterra or Somigliana dislocation [18], and residual elastic deformations manifest within a body that can be treated as locally continuous in $\widetilde{B}$. The corresponding definition for the average residual elastic deformation gradient in Eq. (17) is, in Cartesian coordinates,

$$F^I_{AB} = V^{-1}\int_V x_{(A,B)}dV = \delta_{AB} + V^{-1}\int_V u_{(A,B)}dV \tag{35}$$

Relation (35) is a key definition that will be used repeatedly in what follows. Mapping the self-equilibrium conditions in Eq. (29) to the reference configuration and substituting from Eq. (33),

$$\delta^A_{.a}\delta^B_{.b}\int_v \sigma^{ab}dv = \delta^A_{.a}\delta^B_{.b}\int_V x^b_{.,C}P^{aC}dV = \int_V(\delta^B_{.C} + u^B_{.,C})\frac{\partial\Psi_0}{\partial u_{A,C}}dV = 0 \tag{36}$$

The integral in Eq. (36) becomes, upon substitution of Eq. (34) with omission of terms of orders higher than 3,

$$0 = \int_V(\delta^B_{.C} + u^B_{.,C})\frac{\partial\Psi_0}{\partial u_{A,C}}dV = \int_V \mathbb{C}^{ABCD}u_{C,D}dV + \int_V(\mathbb{C}^{AECD}u^B_{.,E} + \mathbb{C}^{BECD}u^A_{.,E})u_{C,D}dV + \frac{1}{2}\int_V \mathbb{C}^{ABCD}u_{E,C}u^E_{.,D}dV + \frac{1}{2}\int_V \mathbb{C}^{ABCDEF}u_{C,D}u_{E,F}dV \tag{37}$$

Neglecting products of order 2 in displacement gradients in a linear-elastic body with spatially constant moduli, Eq. (37) reduces to

$$\mathbb{C}^{ABCD}\int_V u_{C,D}dV = 0 \rightarrow \int_V u_{(C,D)}dV = 0 \rightarrow F^I_{CD} = \delta_{CD} \tag{38}$$

since $\mathbb{C}^{ABCD}$ is assumed positive definite. Linear elastic approximation (38) states that no average elastic shape or volume change occurs in a homogeneous self-equilibrated body. The latter would be true even if local elastic dilatation from defects does not vanish, as is exhibited in straight line edge dislocation and wedge and twist disclination solutions [6,21] for linear-elastic isotropic bodies. On the other hand, for a nonlinear elastic body with spatially constant moduli, components of the integrated symmetric displacement gradient are given by the six independent integral equations

$$\mathbb{C}^{ABCD}\int_V u_{(C,D)}dV = -\mathbb{C}^{AECD}\int_V u^B_{.,E}u_{C,D}dV - \mathbb{C}^{BECD}\int_V u^A_{.,E}u_{C,D}dV - \frac{1}{2}\mathbb{C}^{ABCD}\int_V u_{E,C}u^E_{.,D}dV - \frac{1}{2}\mathbb{C}^{ABCDEF}\int_V u_{C,D}u_{E,F}dV \tag{39}$$

Hence from Eqs. (35) and (39), components of $\mathbf{F^I}$ may be nonnegligible:

$$F^I_{MN} = \delta_{MN} - V^{-1}\mathrm{S}_{MNAB}\left[\mathbb{C}^{AECD}\int_V u^B_{.,E}u_{C,D}dV + \mathbb{C}^{BECD}\int_V u^A_{.,E}u_{C,D}dV + \frac{1}{2}\mathbb{C}^{ABCD}\int_V u_{E,C}u^E_{.,D}dV + \frac{1}{2}\mathbb{C}^{ABCDEF}\int_V u_{C,D}u_{E,F}dV\right] \tag{40}$$

Rank 4 elastic compliance S_{MNAB} in Eq. (40) satisfies [29,48]

$$2\mathbb{C}^{CDAB}\mathrm{S}_{ABMN} = \delta^C_{.M}\delta^D_{.N} + \delta^D_{.M}\delta^C_{.N} \tag{41}$$

By introducing the quantity

$$\hat{\mathbb{C}}^{CDABEF} = -\mathbb{C}^{ABCD}\delta^{EF} - \mathbb{C}^{ABEF}\delta^{CD} + \mathbb{C}^{AFCD}\delta^{BE} + \mathbb{C}^{BFCD}\delta^{AE} + \mathbb{C}^{EFAD}\delta^{BC} + \mathbb{C}^{EFBD}\delta^{AC} + \mathbb{C}^{ABFD}\delta^{CE} + \mathbb{C}^{ABED}\delta^{CF} + \mathbb{C}^{ABCDEF}, \tag{42}$$

relation (39) can be written more compactly as [44]

$$\mathbb{C}^{ABCD}\int_V u_{(C,D)}dV = \frac{1}{2}\mathbb{C}^{ABCD}\int_V u_{C,E}u^E_{.,D}dV - \mathbb{C}^{ABCD}\int_V u^E_{.,E}u_{C,D}dV - \frac{1}{2}\hat{\mathbb{C}}^{CDABEF}\int_V u_{C,D}u_{E,F}dV \tag{43}$$

Correspondingly, Eq. (40) can be replaced with

$$F^I_{MN} = \delta_{MN} + V^{-1}S_{MNAB}\left[\frac{1}{2}\mathbb{C}^{ABCD}\int_V u_{C,E}u^E_{.,D}dV - \mathbb{C}^{ABCD}\int_V u^E_{.,E}u_{C,D}dV - \frac{1}{2}\hat{\mathbb{C}}^{CDABEF}\int_V u_{C,D}u_{E,F}dV\right] \tag{44}$$

Notice from Eqs. (40) and (44) that both geometric nonlinearity (quadratic terms in displacement gradients) and material nonlinearity (third-order elastic constants) contribute to $\mathbf{F^I}$, and that $\mathbf{F^I}$ does not necessarily reduce to the unit tensor when the third-order constants vanish. If the strain energy in Eq. (34) is extended to incorporate displacement gradients of order higher than 3, e.g., fourth-order elastic constants [48], then the effects of these higher-order terms will likewise enter the right sides of Eqs. (40) and (44). When elastic moduli are not spatially constant, for example, in a multiphase composite or body with foreign inclusions, Eqs. (40) and (44) do not strictly apply since in that case elastic coefficients cannot be moved outside the volume integrals. If V is a polycrystal with randomly oriented grains, then uniform isotropic elastic properties (i.e., effective moduli) can be assigned to each individual crystal as an approximation.

Because the average residual elastic deformation results from nonlinear elastic effects, specifically products of displacement gradients of order 2 in Eqs. (40) and (44), the contribution of the average residual elastic deformation $\mathbf{F^I}$ to the total deformation gradient $\mathbf{F}$ of Eq. (15) will generally be small in conventional engineering applications, wherein defect densities are low to moderate. For example, linear elasticity theory is generally deemed valid beyond some cutoff distance on the order of 1–10 lattice parameters from the dislocation core [29,57], beyond which magnitudes of elastic displacement gradients are small (less than $\sim$0.1) so that contributions from such linear-elastic regions to terms in braces in Eq. (44) will be negligible. On the other hand, for materials with very large dislocation densities in which core regions comprise a substantial fraction of the volume element, nonlinear elastic contributions could be substantial, in which case the difference $\mathbf{F^I}-\mathbf{1}$ would be non-negligible. The contribution of tensile volumetric and deviatoric parts of local elastic displacement gradients to $\mathbf{F^I}$ would also be limited by the theoretical strength of the crystal, typically on the order of 10% of an elastic shear modulus [57], since the material would fracture at elastic strains producing tensile or shear stresses in excess of the theoretical strength. On the other hand, large elastic volumetric compressions are usually sustainable in crystals. The effect of residual elasticity would be greatest in materials whose third-order elastic constants are substantially larger than second-order constants; in some crystalline solids, representative third-order constants can exceed second-order constants by an order of magnitude or more [29].

3.4 Average Residual Elastic Volume Changes. Now consider the average volume change in the body resulting from the field of local residual elastic displacement gradients $u_{A,B}$. The preceding derivations (and those that follow in Sec. 3.4) apply regardless of whether or not the average shape change resulting from $u_{A,B}$ vanishes. However, for a crystal containing a large number of randomly oriented defects (e.g., dislocation and disclination lines and loops), it may be reasonable to assume that the change in dimensions of the crystal imparted by local stress fields of defects exhibits no preferred directions, implying that the crystal undergoes only a volume change and no shape change. The average residual elastic volume change is also of great practical interest because it can be easily measured experimentally for plastically deformed crystals, with results then available to validate the theory. The residual elastic deviatoric shape change, on the other hand, cannot be obtained simply from the deformed shape of a sample of material since it cannot be readily delineated from the macroscopic shape change resulting from dislocation glide.

The change in a differential volume of a body in coincident spatial and reference coordinate systems is measured by [44]

$$dv/dV = \det(\delta^A_B + u^A_{.,B}) = \tfrac{1}{6}[(x^A_{.,A})^3 - 3x^A_{.,A}x^B_{.,C}x^C_{.,B} + 2x^B_{.,C}x^C_{.,A}x^A_{.,B}] = 1 + u^A_{.,A} + \tfrac{1}{2}(u^A_{.,A})^2 - \tfrac{1}{2}u^A_{.,B}u^B_{.,A} \tag{45}$$

where terms of order 3 and higher in displacement gradients are neglected in the final equality. In the present application in the context of Fig. 1, dv is the volume of a differential subelement of the body in configuration $\bar{B}$, and dV is the volume of that subelement in $\tilde{B}$. Integrating Eq. (45), a second-order accurate measure of the net volume change attributed to residual elastic deformation within the crystal is

$$\Delta V = \int_V u^A_{.,A}dV + \frac{1}{2}\int_V [(u^A_{.,A})^2 - u^A_{.,B}u^B_{.,A}]dV \tag{46}$$

The right sides of Eqs. (40), (44), and (46) depend on local residual elastic displacement gradient fields in the body. For crystals of high symmetry, these relations can be further reduced by appealing to particular forms of the elastic coefficients. Specifically, for cubic crystal systems of the highest symmetry (Laue group CI), second-order moduli consist of three independent coefficients and the third-order moduli of six independent coefficients. Consider a coordinate system with axes parallel to the cube axes of the crystal. In Voigt's notation [58], pairs of indices $11\rightarrow1$, $22\rightarrow2$, $33\rightarrow3$, $23\rightarrow4$, $13\rightarrow5$, $12\rightarrow6$, and $2E_{AB}\rightarrow E_\alpha(1+\delta_{AB})$, where Greek indices span $\alpha=1,2,\ldots,6$, nonzero second-order constants are

$$C_{11}=C_{22}=C_{33},\quad C_{12}=C_{13}=C_{23},\quad C_{44}=C_{55}=C_{66} \tag{47}$$

and nonzero third-order constants are

$$C_{111}=C_{222}=C_{333},\quad C_{144}=C_{255}=C_{366},$$
$$C_{112}=C_{113}=C_{122}=C_{223}=C_{133}=C_{233},\quad C_{123}, \tag{48}$$
$$C_{155}=C_{166}=C_{244}=C_{266}=C_{344}=C_{355},\quad C_{456}$$

The following notation is common [11]:

$$3B = C_{11}+2C_{12},\quad 2G = C_{11}-C_{12},\quad -2G' = C_{11}-C_{12}-2C_{44} \tag{49}$$

where B is the bulk modulus and G and G' are the shear moduli. In a cubic crystal, the first term on the right of Eq. (34) can be written as [44]

$$\begin{aligned} W &= \tfrac{1}{2}\mathbb{C}^{ABCD}u_{A,B}u_{C,D} = \tfrac{1}{2}B(u^A_{.,A})^2 \\ &\quad + G[(u^A_{.,B}u^B_{.,A} + u^A_{.,B}u^{;B}_{A})/2 - (u^A_{.,A})^2/3] \\ &\quad + G'[(u^A_{.,B}u^B_{.,A} + u^A_{.,B}u^{;B}_{A})/2 - (u^1_{.,1})^2 - (u^2_{.,2})^2 - (u^3_{.,3})^2] \\ &= W_D + W_S + W'_S \end{aligned} \tag{50}$$

where W_D is the strain energy of dilatation, and W_S and W'_S result from shape changes of the crystal. In an isotropic material (e.g., a polycrystal with no preferred orientations), the number of constants in Eq. (47) is further reduced to 2 according to

$$2C_{44} = C_{11} - C_{12} \tag{51}$$

and in Eq. (48) reduced to 3 according to

$$2C_{144} = C_{112} - C_{123}, \quad 4C_{155} = C_{111} - C_{112}$$
$$8C_{456} = C_{111} - 3C_{112} + 2C_{123} \tag{52}$$

Thus in an isotropic material, B and G of Eq. (49), and W_D and W_S of Eq. (50) are unchanged, $G'=0$ in Eq. (49), and $W'_S=0$ in Eq. (50). Summing over the first two indices of Eq. (39), and using the first of Eq. (50) gives

$$\mathbb{C}^{A.CD}_{.A}\int_V u_{(C,D)}dV = -4\int_V W dV - \frac{1}{2}\mathbb{C}^{A.CD}_{.A}\int_V u_{E,C}u^E_{.,D}dV - \frac{1}{2}\mathbb{C}^{A.CDEF}_{A}\int_V u_{C,D}u_{E,F}dV \tag{53}$$

Appealing to Eq. (43),

$$\mathbb{C}^{A.CD}_{.A}\int_V u_{(C,D)}dV = -3\int_V W dV + \frac{1}{2}\mathbb{C}^{A.CD}_{.A}\int_V (u_{C,E}u^E_{.,D} - u_{C,D}u^E_{.,E})dV - \frac{1}{2}\hat{\mathbb{C}}^{A.CDEF}_{A}\int_V u_{C,D}u_{E,F}dV \tag{54}$$

For a cubic crystal satisfying Eqs. (47)–(50), this reduces to

$$3B\int_V u^D_{.,D}dV = -3\int_V W dV - \frac{3}{2}B\int_V [(u^A_{.,A})^2 - u^A_{.,B}u^B_{.,A}]dV - \frac{1}{2}\hat{\mathbb{C}}^{A.CDEF}_{A}\int_V u_{C,D}u_{E,F}dV \tag{55}$$

Then from Eq. (46), the net volume change for the element of reference volume V is

$$\Delta V = -\frac{1}{B}\int_V W dV - \frac{1}{6B}\hat{\mathbb{C}}^{A.CDEF}_{A}\int_V u_{C,D}u_{E,F}dV \tag{56}$$

Letting $\det(x^a_{.,A})=\upsilon$, where $\upsilon>0$, the rightmost term of Eq. (56) can be written as [44]

$$\frac{1}{6}\hat{\mathbb{C}}^{A.CDEF}_{A}\int_V u_{C,D}u_{E,F}dV = \frac{\upsilon}{B}\frac{\partial B}{\partial \upsilon}\int_V W_D dV + \frac{\upsilon}{G}\frac{\partial G}{\partial \upsilon}\int_V W_S dV + \frac{\upsilon}{G'}\frac{\partial G'}{\partial \upsilon}\int_V W'_S dV \tag{57}$$

Setting $\partial/\partial\upsilon = -(B/\upsilon)\partial/\partial p$, where p is the Cauchy pressure, and substituting Eqs. (50) and (57) into Eq. (56),

$$\Delta V = \frac{1}{B}\left[\left(\frac{\partial B}{\partial p}-1\right)\int_V W_D dV + \left(\frac{B}{G}\frac{\partial G}{\partial p}-1\right)\int_V W_S dV + \left(\frac{B}{G'}\frac{\partial G'}{\partial p}-1\right)\int_V W'_S dV\right] \tag{58}$$

where moduli B, G, and G' and their derivatives with respect to pressure are all evaluated at a stress-free reference state. After defining average strain energies on a per-reference-volume basis as

$$\overline{W}_D = V^{-1}\int_V W_D dV, \quad \overline{W}_S = V^{-1}\int_V W_S dV, \quad \overline{W}'_S = V^{-1}\int_V W'_S dV \tag{59}$$

and the quantity

$$\overline{J} = 1 + \Delta V/V \tag{60}$$

the normalized volume change for a self-equilibrated, cubic nonlinear elastic solid is found as

$$\overline{J} = 1 + \frac{1}{B}\left[\left(\frac{\partial B}{\partial p}-1\right)\overline{W}_D + \left(\frac{B}{G}\frac{\partial G}{\partial p}-1\right)\overline{W}_S + \left(\frac{B}{G'}\frac{\partial G'}{\partial p}-1\right)\overline{W}'_S\right] \tag{61}$$

If the cubic second-order elastic coefficients, their pressure derivatives, and each of the average strain energy densities of Eq. (59) are known, normalized residual volumetric deformation can be computed from Eq. (61). If strain energy densities are all positive, and if coefficients of the energy densities in Eq. (61) are all of the same sign (e.g., positive), then the overall volume change will be of that sign (e.g., positive). If only the total strain energy density $\overline{W}=\overline{W}_D+\overline{W}_S+\overline{W}'_S$ is known, for example, from experiments [11,45], then Eqs. (50) and (61) can be combined to establish bounds on the normalized volume change [44]. Such bounds have been validated for several polycrystalline cubic metals [11], wherein the volume changes were always found positive by theory and experiment. For an isotropic solid, Eq. (61) reduces to

$$\overline{J} = 1 + \frac{1}{B}\left(\frac{\partial B}{\partial p}-1\right)\overline{W}_D + \frac{1}{G}\left(\frac{\partial G}{\partial p}-\frac{G}{B}\right)\overline{W}_S \tag{62}$$

In an isotropic body, pressure derivatives of tangent bulk and shear moduli B and G in the undistorted reference configuration are related to third-order elastic constants by [29]

$$-B\left.\frac{\partial B}{\partial p}\right|_{p=0} = \mathrm{C}_{123} + 2\mathrm{C}_{144} + \frac{8}{9}\mathrm{C}_{456}$$
$$-B\left.\frac{\partial G}{\partial p}\right|_{p=0} = B + \frac{1}{3}G + \mathrm{C}_{144} + \frac{4}{3}\mathrm{C}_{456} \tag{63}$$

Formula (61) for cubic crystals is attributed to Toupin and Rivlin [44], while Eq. (62) was developed earlier by Zener [8]. Isotropic formula (62) for the case when the dilatational energy vanishes agrees with that of Holder and Granato [10] obtained by simple thermodynamic arguments:

$$\Delta V/V = \frac{\partial g}{\partial p} = \frac{1}{G_e}\left(\frac{\partial G_e}{\partial p}-\frac{G_e}{B}\right)g = \frac{1}{G_e}\left(\frac{\partial G_e}{\partial p}-\frac{G_e}{B}\right)E\rho_T \tag{64}$$

where g is the Gibbs free energy change from defects, per unit reference volume that depends on pressure p and temperature θ, and G_e is an effective elastic constant that depends on the mathematical form of the strain energy of the particular defect. In the final term of Eq. (64), E is the elastic strain energy per unit length of the defect, and ρ_T is the total length per unit volume of the defect. For a number of metallic crystals, Holder and Granato [10] found that delineation of dilatational and deviatoric energies and effects of anisotropy had little effect on volume changes from straight dislocations predicted using Eq. (64).

The source of the local displacement gradient and residual strain energy in the body to this point has been arbitrary, so long as Eqs. (20), (23), and (34) apply; that is, traction is continuous across all internal surfaces, the body is self-equilibrated such that external traction is absent, and the crystal's local constitutive response is described by hyperelasticity with terms of order higher than 3 in the displacement gradients neglected in the strain energy. Defects induce such displacement gradients and residual strain energies. These may include, for example, dislocation and disclination lines and loops, stacking faults, grain boundaries, twin

boundaries, and slip bands. On the other hand, volume changes attributed to point defects (e.g., substitutional atoms, interstitials, and vacancies), phase transformations, voids, and open cracks are not considered in the present treatment, since dimensional changes computed according to the present theory account only for volume and shape changes resulting from stress fields of defects and not volume and shape changes associated with defects themselves. However, the additional volume change induced by a point defect—the volume change in addition to the misfit dilatation in a sphere-in-hole model—attributed to elastic nonlinearity can be estimated from Eq. (62) for an isotropic elastic body [19]. Anisotropy cannot be directly addressed in Eq. (61) to describe the effects of defects wherein moduli may change with position, for example, grain boundaries and twin boundaries across which lattice orientations may differ. However, isotropic approximation (62) could be used as an estimate in these cases, as in previous applications toward polycrystals [43] and single crystals of lower symmetry [15].

Also neglected in the foregoing continuum elastic analysis are explicit effects of defect cores on residual deformation. For example, elastic strain, stress, and strain energies imparted by Volterra line defects diverge as the radial distance from the line shrinks to zero [6], and even nonlinear elasticity is inadequate for describing the nonconvex energy distribution imparted by the highly distorted crystal structure within defect cores. In the present treatment, one can imagine each defect line to be surrounded by a traction-free cylindrical boundary delineating the core volume from the surrounding elastic continuum of reference volume V. In linear elasticity, stresses and strains resulting from traction acting on the cylindrical boundary decay as R^{-3}, where R is the distance from the defect line, and hence are usually neglected [29]. The elastic continuum is self-equilibrated in this approximation, and Eq. (36) applies.

3.5 Straight Edge and Screw Dislocations. Consider volume changes imparted by dislocation lines in the isotropic approximation. The energy per unit length (linear-elastic energy plus core and interaction energies) of a straight dislocation in an infinite isotropic medium is written

$$\overline{E} = \frac{Gb^2}{4\pi K}\ln\left(\frac{R}{R_C}\right) + \hat{E}, \quad K = \begin{cases} 1-\nu & \text{(edge dislocation)} \\ 1 & \text{(screw dislocation)} \end{cases} \tag{65}$$

where b is the magnitude of the Burgers vector, $\nu=(3B-2G)/(6B+2G)$ is Poisson's ratio, R is the radial distance from the dislocation core, R_C is the radius of the dislocation core, and $\hat{E}$ is a correction that accounts for core energy, line curvature, interaction energies from other defects and boundaries, and stacking faults associated with partial dislocations.

Denoted by $E^E=\overline{E}-\hat{E}$ is the elastic strain energy density per unit line length L of straight, noninteracting edge dislocations, separated into dilatational and shear contributions as [43]

$$E_D^E = \frac{Gb^2}{12\pi}\frac{1-\nu-2\nu^2}{(1-\nu)^2}\ln\left(\frac{R}{R_C}\right), \quad E_S^E = \frac{Gb^2}{12\pi}\frac{2-2\nu+2\nu^2}{(1-\nu)^2}\ln\left(\frac{R}{R_C}\right) \tag{66}$$

Letting

$$\overline{W}_D V = E_D^E L, \quad \overline{W}_S V = E_S^E L \tag{67}$$

and multiplying Eq. (62) by V/L, the volume change per unit length of edge dislocation line is [29,43]

$$\left.\frac{\Delta V}{L}\right|_{\text{edge}} = \frac{1}{B}\left(\frac{\partial B}{\partial p}-1\right)E_D^E + \frac{1}{G}\left(\frac{\partial G}{\partial p}-\frac{G}{B}\right)E_S^E = \frac{E^E}{3}\left[\frac{1-\nu-2\nu^2}{(1-\nu)B}\left(\frac{\partial B}{\partial p}-1\right)+\frac{2-2\nu+2\nu^2}{(1-\nu)G}\left(\frac{\partial G}{\partial p}-\frac{G}{B}\right)\right] \tag{68}$$

where $E^E=E_D^E+E_S^E$ is the total elastic line energy of an edge dislocation.

Analogously, as denoted by $E^S=\overline{E}-\hat{E}$, the strain energy per unit line length L of straight, noninteracting screw dislocations, partitioned as [43]

$$E_D^S = 0, \quad E_S^S = \frac{Gb^2}{4\pi}\ln\left(\frac{R}{R_C}\right) \tag{69}$$

Letting

$$\overline{W}_S V = E_S^S L = E^S L \tag{70}$$

where E^S is the total elastic line energy of a screw dislocation, and multiplying Eq. (62) by V/L, the volume change per unit length of straight screw dislocation lines is [29,43]

$$\left.\frac{\Delta V}{L}\right|_{\text{screw}} = \frac{E^S}{G}\left(\frac{\partial G}{\partial p}-\frac{G}{B}\right) \tag{71}$$

Now let the total dislocation line density per unit reference volume be given by the sum

$$\rho_T = L/V = \rho_E + \rho_S \tag{72}$$

where now L is the total length of edge and screw dislocations in volume V, ρ_E is the density of edge dislocations, and ρ_S is the density of screw dislocations. Define from Eq. (65)

$$E_T = KE^E = E^S = \frac{Gb^2}{4\pi}\ln\left(\frac{R}{R_C}\right) \tag{73}$$

and let $\chi=\rho_E/\rho_T$ be the fraction of pure edge dislocations in the total dislocation density. Superposing volume changes from Eqs. (68) and (71), and using Eq. (72), Eq. (62) becomes

$$\overline{J} = 1 + \rho_E \left.\frac{\Delta V}{L}\right|_{\text{edge}} + \rho_S \left.\frac{\Delta V}{L}\right|_{\text{screw}} = 1 + \left\{\frac{\chi}{3K}\left[\frac{1-\nu-2\nu^2}{(1-\nu)B}\left(\frac{\partial B}{\partial p}-1\right)+\frac{2-2\nu+2\nu^2}{(1-\nu)G}\left(\frac{\partial G}{\partial p}-\frac{G}{B}\right)\right] + \frac{1-\chi}{G}\left(\frac{\partial G}{\partial p}-\frac{G}{B}\right)\right\}E_T\rho_T \tag{74}$$

Relation (74) yields the volume change associated with straight, noninteracting pure screw and edge dislocation lines in an isotropic body with homogeneous elastic properties. While terms in braces in Eq. (74) include nonlinear elastic effects (i.e., pressure derivatives of the elastic moduli or third-order elastic constants from Eq. (63)), dislocation line energy E_T does not account explicitly for nonlinearity or energy of dislocation cores. Thus, Eq. (74) represents the product of third-order nonlinear elasticity (terms in braces) and linear elasticity (defect energy). Products of purely linear-elastic origin would yield null volume change, as implied by Eq. (38), while higher-order products of nonlinear origin (e.g., products of pressure derivatives of moduli with contributions of nonlinear elasticity to dislocation energies) are neglected. Relation (74) can be used directly to compute the volume change in a (poly)crystal if line densities of edge and screw dislocations, their energies per unit length, and the requisite elastic constants are known. The preceding analysis assumes that defect densities are negligible in the reference configuration. When dislocation densities are substantial in the initial state, the predicted volume change between the initial and final configurations corresponds only to the change in defect density that occurs during

deformation, rather than that associated with the absolute density of dislocations.

Dislocation line densities in the preceding developments are defined per unit reference volume (equivalent in configurations B_0 and $\tilde{B}$ of Fig. 1). When the dislocation line density ρ_T is measured in the externally unloaded but internally stressed configuration $\bar{B}$, then $\rho_T \rightarrow \bar{J}\rho_T$ in Eq. (74) such that

$$\bar{J}^{-1} = 1 - \left\{ \frac{\chi}{3K}\left[\frac{1-\nu-2\nu^2}{(1-\nu)B}\left(\frac{\partial B}{\partial p}-1\right) + \frac{2-2\nu+2\nu^2}{(1-\nu)G}\left(\frac{\partial G}{\partial p}-\frac{G}{B}\right)\right] + \frac{1-\chi}{G}\left(\frac{\partial G}{\partial p}-\frac{G}{B}\right)\right\} E_T \rho_T \tag{75}$$

However, the distinction between configurations used to define the dislocation line density will have a trivial effect on computed values of $\bar{J}$ for small volume changes $(1+\Delta V/V \approx 1/(1-\Delta V/V))$, and in these cases preferential use of Eq. (75) over Eq. (74) is probably not warranted given the uncertainty in dislocation densities that can be measured experimentally. The dislocation line energy in Eq. (73) depends on the core radius R_C and the cutoff radius R. A typical approximation is [57]

$$E_T = \alpha G b^2 \tag{76}$$

with $0.5 \leq \alpha = \ln(R/R_C)/4\pi \leq 1.0$. Introducing the dimensionless quantities

$$A_E = \frac{E_T \rho_T}{3K}\left[\frac{1-\nu-2\nu^2}{(1-\nu)B}\left(\frac{\partial B}{\partial p}-1\right) + \frac{2-2\nu+2\nu^2}{(1-\nu)G}\left(\frac{\partial G}{\partial p}-\frac{G}{B}\right)\right] \tag{77}$$

$$A_S = \frac{E_T \rho_T}{G}\left(\frac{\partial G}{\partial p}-\frac{G}{B}\right)$$

the volume change in Eq. (74) becomes

$$\Delta V/V = \bar{J} - 1 = A_E \chi + A_S(1-\chi) \tag{78}$$

Thus, $\Delta V/V$ for a mixture of straight, noninteracting edge and screw dislocations will fall between the volume change A_E resulting from the same density of pure edge dislocations and the volume change A_S resulting from the same density of pure screw dislocations.

3.6 Approximate Volume Changes. Returning to the overall dimensional changes of the body induced by averaged local displacement gradients, consider Eq. (35). Defining the quantities

$$\bar{K} = V^{-1}\int_V u^A_{.,A} dV, \quad \bar{L^2} = V^{-2}\int_V u^A_{.,B} dV \int_V u^B_{.,A} dV \tag{79}$$

and neglecting terms of orders 3 and higher in displacement gradients, the analog of Eq. (45) is

$$\det(F^I_{AB}) = 1 + \bar{K} + \bar{K}^2/2 - \bar{L^2}/2 \tag{80}$$

Recall from Eqs. (46) and (60) that

$$\bar{J} = 1 + \bar{K} + \frac{1}{2}\int_V [(u^A_{.,A})^2 - u^A_{.,B}u^B_{.,A}]dV \tag{81}$$

Thus,

$$\bar{J} = \det(F^I_{AB}) - \frac{1}{2}(\bar{K^2} - \bar{L^2}) + \frac{1}{2}\int_V [(u^A_{.,A})^2 - u^A_{.,B}u^B_{.,A}]dV \tag{82}$$

so that at least to first-order in displacement gradients, $\bar{J} = \det(F^I_{AB})$. Possible differences between $\bar{J}$ and $\det(F^I_{AB})$ may arise because the determinant operation and volume integration do not commute. When products of displacement gradients and their averages are small, $F^{IA}_{.A} - \delta^A_{.A} = \bar{K} \approx \det(F^I_{AB}) - 1$ and $\bar{J} \approx \det(F^I_{AB})$. Recall that $F^I_{AB} = F^I_{(AB)}$ is a stretch with no rotation. Even though in some cases defects impart no local dilatation in the linear-elastic approximation (e.g., Volterra screw dislocations in isotropic solids), a volume change can still result (e.g., Eq. (71)) because of nonlinear elastic effects.

3.7 Examples. Table 1 presents strain energies per unit line length E of a number of defects: straight edge and screw dislocations discussed already in Sec. 3.5; circular screw and prismatic dislocation loops of radius R and core radius R_C, and straight wedge disclinations and circular twist and wedge disclination loops of Frank vector ω, radius r, and core radius r_C. Energies all correspond to defects in infinite, isotropic linear-elastic solids. Analytical formulas for energies follow from references quoted in Table 1, while normalized volume changes $(\Delta V/V)/(\rho_T a^2)$ computed for copper follow from Eq. (68) for edge dislocations and from Eq. (62) for the other defects, using material properties listed in Table 2. For defects besides edge dislocations, strain energy is treated as deviatoric, leading to the linear relationship between volume change and defect density given in Eq. (64). This is a rigorous assertion for screw dislocation loops and twist disclination loops but not prismatic loops or wedge disclinations, though it has been used elsewhere for these defects [18,61] and should provide a reasonable approximation to the volume change for many metals [10], including Cu. Again, ρ_T is the line length per unit reference volume of the defect, and a is the lattice spacing of the conventional unit cell in a perfect crystal at room temperature. Experimental results for polycrystalline Cu are provided for comparison [45]; the range of volume changes reported in Table 1 for the experiments corresponds to estimates of dislocation line length from energy measurements after plastic compressive strains ranging from 0.3 to 0.7. The nature of the defects (e.g., edge versus screw and straight lines versus loops) was not reported in that experimental investigation.

From Table 1, the normalized volume changes predicted for various kinds of dislocations agree with the experimental findings within a factor of ~ 2 and are very close for edge dislocations and prismatic loops. Volume changes per unit defect length in Cu are positive (i.e., defects cause expansion) and small. For example, a 1% volume increase would require an immense density of edge dislocations on the order of $\rho_T \sim 0.01 a^{-2} \sim 10^{17}$ m^{-2}, corresponding to an average dislocation spacing on the order of $10a$. For small volume changes $(\Delta V/V < 1\%)$, $\det \mathbf{F^I}$ should be expected provide an accurate approximation of $\bar{J}$ according to Eq. (82). Disclination energies and volume changes are comparable to those for dislocations for the small cutoff radii or small loops considered here $(r = 10 r_C)$ but would diverge quickly at large distances r from the core of straight disclinations or for larger disclination loops. Elastic anisotropies of individual grains, defect core energies, and interaction energies among defects and between defects and the external boundary of the body (e.g., image forces) are neglected in this application of the model; such effects presumably contribute to discrepancies between theory and experiment.

The results of Table 1, along with experimental data summarized by Wright [11], suggest that volume changes resulting from residual elasticity associated with dislocations should be small in metallic crystals of cubic symmetry deformed in compression or shear to strains on the order of unity, under quasistatic conditions. The experimental results in Table 1 [45] correspond to dislocation densities on the order of $\rho_T \sim 10^{15}$ m^{-2}, leading to volume changes on the order of $\Delta V/V \sim 10^{-4}$. Such small volume changes would seem inconsequential in the context of measured yield properties of materials in unconfined loading, when specimens are free to expand or contract laterally. However, under lateral confinement, for example, uniaxial strain conditions occurring in shock loading [14,15], small volume changes can drastically affect the measured hydrostatic pressure. Volume changes cannot be accommodated by dislocation glide, as noted in Sec. 2.1; hence,

Table 1 Defect energies and residual volume changes in copper

Defect	Energy/length E (nJ/m)	Volume change $(\Delta V/V)/(\rho_T a^2)$
Edge dislocation[a]: $E=\frac{Gb^2}{4\pi(1-\nu)}\ln\frac{R}{R_C}$	5.29	0.89
Screw dislocation[a]: $E=\frac{Gb^2}{4\pi}\ln\frac{R}{R_C}$	3.39	0.51
Screw dislocation loop[b]: $E\approx\frac{Gb^2}{12\pi(1-\nu)}\left[3(1-\nu)\ln\frac{8R}{R_C}-(9-10\nu)\right]$	3.21	0.49
Prismatic dislocation loop[b]: $E\approx\frac{Gb^2}{4\pi(1-\nu)}\left[\ln\frac{8R}{R_C}-2\right]$	5.32	0.81
Wedge disclination[c]: $E=\frac{G\omega^2r^2}{16\pi(1-\nu)}\left[1-\left(\frac{r_C}{r}\right)^2-4\left(\frac{r_C}{r}\right)^2\left(1-\left(\frac{r_C}{r}\right)^2\right)^{-1}\ln^2\left(\frac{r_C}{r}\right)\right]$	4.24	0.64
Twist disclination loop[c]: $E\approx\frac{G\omega^2r^2}{4\pi}\left[\ln\frac{8r}{r_C}-\frac{8}{3}\right]$	15.8	2.4
Wedge disclination loop[d]: $E\approx\frac{G\omega^2r^2}{8\pi(1-\nu)}\left[\ln\frac{8r}{r_C}-\frac{8}{3}\right]$	12.4	1.9
Experiment[e]	–	0.8–1.1

[a]Reference [21].
[b]Reference [59].
[c]Reference [60].
[d]References [61,62].
[e]Reference [45].

any residual inelastic volume increase must be compensated by an elastic volume decrease and corresponding hydrostatic pressure. Extremely high dislocation densities, $\rho_T \sim 10^{16}$ m^{-2}, have been observed for metals such as Cu deformed in shock conditions [14]. A dislocation density of 10^{16} m^{-2} would lead to an expansion on the order of 0.1%, which would in turn require an offsetting pressure on the order of 0.1% of the bulk modulus, or $\sim$0.15 GPa in Cu. Such contributions of defects to pressure or volume change would manifest implicitly in the measured equation of state (i.e., pressure-volume-temperature relationship), bulk modulus, and pressure derivatives of the bulk modulus obtained from high-pressure experiments. Substantial effects of large dislocation densities on tangent elastic moduli of metallic single crystals deformed in uniaxial strain have been predicted using atomistic methods [51]. Very large dislocation densities comprising dislocation walls in subdivided grains have been observed in metals subject to severe plastic deformation [63]; residual elastic volume changes could be significant in highly defective regions of such materials.

While closed-form analytical solutions are not available for the deviatoric part of $\mathbf{F^I}$, magnitudes of its deviatoric components are expected to be on the same order as its volumetric part, i.e., small except in cases where defect densities are extremely large. Meant by small are conditions $F^I_{AB}-\delta_{AB}<0.001$ for defect densities $\rho_T < 10^{15}$ m^{-2} in cubic metals such as copper, though larger residual elastic deformations would be expected in crystals that feature stronger pressure sensitivity of the elastic coefficients. Because deviatoric deformation can be accommodated by plastic slip, there seems to be no capacity available to delineate contributions from residual elasticity versus dislocation flux to the plastic properties of materials (e.g., yield and flow properties) measured in experiments on single or polycrystals. The effect of $\mathbf{F^I}$ is implicitly included in such experimental measurements. The effects of $\mathbf{F^I}$ could in principle be delineated via numerical simulations incorporating atomistic or discrete dislocation dynamics. Presumably, contributions of residual elasticity to overall deformation gradient $\mathbf{F}$ are small in conventional engineering applications wherein defect densities are small to moderate, since omission of $\mathbf{F^I}$ in standard crystal plasticity models [53] does not seem to inhibit accu-

Table 2 Properties for copper[a]

G (GPa)	B (GPa)	ν	$\partial G/\partial p$	$\partial B/\partial p$	a (nm)	b (nm)	r (nm)	ω	R_C (nm)	R/R_C	r/r_C
47	152	0.36	0.8	4.4	0.362	0.256	1.0	$\pi/2$	1.0	10^6	10

[a]Reference [43] (elastic coefficients and their pressure derivatives).

racy of such models. On the other hand, interacting stress fields of dislocations strongly affect yield and strain hardening [57]; furthermore, spatial gradients of $\mathbf{F}^{\mathbf{I}}$ need not always be small even if $\mathbf{F}^{\mathbf{I}}$ itself is small relative to the unit tensor. Gradients of residual elastic deformation, in addition to gradients of lattice rotation [30], can be associated with the density of geometrically necessary dislocations and kinematic hardening in metals [34,35].

4 Atomistic Approach

The volume element of the crystalline solid is now treated as a collection $\mathcal{L}$ of discrete atoms rather than a continuum. Prior to discussion in Sec. 4.4 of the self-equilibrated, relaxed intermediate configuration and means to compute $\mathbf{F}^{\mathbf{I}}$ entering Eq. (17) atomically, relevant background discussion pertinent to lattice statics, atomic stress measures, and atomic interactions are provided in Secs. 4.1–4.3.

4.1 Lattice Statics. The atoms occupy a perfect lattice in the volume element corresponding to configuration B_0 of Fig. 1. As noted already in Eq. (1), the position of each atom i in configuration B_0 is expressed by vector $\mathbf{R}_{\langle i\rangle}$, with angular brackets used to denote the atomic labels. The position vector of atom i in current configuration B is $\mathbf{r}_{\langle i\rangle}$. In classical Newtonian mechanics described via rectangular Cartesian coordinates, the balance of linear momentum for particle i is

$$m_{\langle i\rangle}\ddot{r}^a_{\langle i\rangle} = \hat{f}^a_{\langle i\rangle} + f^a_{\langle i\rangle} \tag{83}$$

where $m_{\langle i\rangle}$ is the mass of atom i, $\hat{f}^a_{\langle i\rangle}$ are the external forces that may be explicitly time dependent, and $f^a_{\langle i\rangle}$ are the conservative forces satisfying

$$f^a_{\langle i\rangle} = -\delta^{ab}\frac{\partial\Phi}{\partial r^b_{\langle i\rangle}} \tag{84}$$

Potential energy Φ is a function of all atomic coordinates:

$$\Phi = \Phi(\mathbf{r}_{\langle i\rangle})_{i\in\mathcal{L}} \tag{85}$$

In the context of lattice statics, external and internal forces balance. In the absence of external forces,

$$\frac{\partial\Phi}{\partial r^b_{\langle i\rangle}} = 0 \tag{86}$$

meaning that the vector sum of all interatomic forces acting on atom i is zero. A more specific form of the potential that maintains translational invariance of the energy depends only on the relative separation between each pair of atoms $\mathbf{r}_{\langle ij\rangle} = \mathbf{r}_{\langle j\rangle} - \mathbf{r}_{\langle i\rangle}$:

$$\Phi = \Phi(\mathbf{r}_{\langle ij\rangle})^{i,j\in\mathcal{L}}_{i\neq j} \tag{87}$$

leading to

$$f^a_{\langle ij\rangle} = \delta^{ab}\frac{\partial\Phi}{\partial r^b_{\langle ij\rangle}} \tag{88}$$

with $f^a_{\langle ij\rangle}$ components of an interaction force between atoms i and j. In general, Eq. (87) accounts for three-body and higher-order interactions, for example, angles subtended by vectors $\mathbf{r}_{\langle ij\rangle}$ among interacting sets of three or more atoms. For materials featuring central force interactions only, Eqs. (87) and (88) reduce to

$$\Phi = \Phi(r_{\langle ij\rangle})^{i,j\in\mathcal{L}}_{i\neq j}, \quad r_{\langle ij\rangle} = (\mathbf{r}_{\langle ij\rangle}\bullet\mathbf{r}_{\langle ij\rangle})^{1/2}, \quad \mathbf{f}_{\langle ij\rangle} = \frac{\partial\Phi}{\partial r_{\langle ij\rangle}}\frac{\mathbf{r}_{\langle ij\rangle}}{r_{\langle ij\rangle}} \tag{89}$$

4.2 Atomic Stress Measures. A number definitions of stress based on atomic quantities have been suggested [46,50,64]. In the context of lattice statics (i.e., null atomic velocities and accelerations), the average virial stress for a group of atoms is often considered equivalent to the average Cauchy stress [46]:

$$\boldsymbol{\sigma} = \frac{1}{2\Omega}\sum_{i\neq j}\mathbf{r}_{\langle ij\rangle}\otimes\mathbf{f}_{\langle ij\rangle} \tag{90}$$

where Ω is the total volume occupied by the group $\mathcal{L}$ of atoms, i.e., the sum of all atomic volumes, in spatial configuration B. The summation in Eq. (90) is, in fact, a double sum, proceeding over all pairs of distinct $(i\neq j)$ atoms. The factor of 2 arises in Eq. (90) because in the notation used here, summation proceeds over all $i\neq j$, $\mathbf{r}_{\langle ij\rangle} = -\mathbf{r}_{\langle ji\rangle}$, and $\mathbf{f}_{\langle ij\rangle} = -\mathbf{f}_{\langle ji\rangle}$. For systems with central force interactions only, symmetry of the stress tensor follows trivially from Eqs. (89) and (90):

$$\sigma^{ab} = \frac{1}{2\Omega}\sum_{i\neq j}\frac{1}{r_{\langle ij\rangle}}\frac{\partial\Phi}{\partial r_{\langle ij\rangle}}r^a_{\langle ij\rangle}r^b_{\langle ij\rangle} = \frac{1}{2\Omega}\sum_{i\neq j}\frac{1}{r_{\langle ij\rangle}}\frac{\partial\Phi}{\partial r_{\langle ij\rangle}}r^b_{\langle ij\rangle}r^a_{\langle ij\rangle} = \sigma^{ba} \tag{91}$$

Now consider a homogeneous deformation $\mathbf{F}$ applied to all atoms in $\mathcal{L}$, leading to $\mathbf{r}_{\langle ij\rangle} = \mathbf{F}\mathbf{R}_{\langle ij\rangle}$ [22,38], with $\mathbf{R}_{\langle ij\rangle} = \mathbf{R}_{\langle j\rangle} - \mathbf{R}_{\langle i\rangle}$ fixed separations between atoms of the reference lattice. Rigid body translations are omitted in this homogeneous deformation. Letting the average strain energy per unit reference volume of the lattice Ψ satisfy $\Omega_0\Psi(\mathbf{F}) = \Phi(\mathbf{r}_{\langle ij\rangle}(\mathbf{F},\mathbf{R}_{\langle ij\rangle}))$, the analog of Eq. (33) is

$$P^{aA} = \frac{\partial\Psi}{\partial F_{aA}} = \frac{1}{2\Omega_0}\sum_{i\neq j}\frac{\partial\Phi}{\partial r^b_{\langle ij\rangle}}\frac{\partial r^b_{\langle ij\rangle}}{\partial F_{aA}} = \frac{1}{2\Omega_0}\sum_{i\neq j}\delta^{ab}\frac{\partial\Phi}{\partial r^b_{\langle ij\rangle}}R^A_{\langle ij\rangle} \tag{92}$$

where Ω_0 is the total volume occupied by the atomic system in B_0. (The atomic volume in a perfect lattice is equal to Ω_0 divided by the number of atoms comprising $\mathcal{L}$.) Relation (92) is a consequence of the affine deformation of all atoms that results in $\partial r^b_{\langle ij\rangle}/\partial F_{aA} = \delta^{ab}R^A_{\langle ij\rangle}$. The average atomic Cauchy stress or average static virial stress is then

$$\begin{aligned}\sigma^{ab} &= \det(F^{-1A}_{\cdot a})P^{bA}F^a_{\cdot A} = \frac{\Omega_0}{\Omega}\left(\frac{1}{2\Omega_0}\sum_{i\neq j}\delta^{bc}\frac{\partial\Phi}{\partial r^c_{\langle ij\rangle}}R^A_{\langle ij\rangle}\right)F^a_{\cdot A}\\ &= \frac{1}{2\Omega}\sum_{i\neq j}r^a_{\langle ij\rangle}\delta^{bc}\frac{\partial\Phi}{\partial r^c_{\langle ij\rangle}}\end{aligned} \tag{93}$$

in agreement with Eq. (90). The present analysis applies only to materials described by potentials of the general form (87) and for which stress relations (90), (92), and (93) are appropriate. For example, metals that can be modeled by combinations of pair potentials and multibody potentials such as the embedded atom method are included. Not admitted are piezoelectric crystals (e.g., noncentrosymmetric ionic solids), some of whose atoms (sublattices) may display a relative shift when polarized, and for which hyperelastic relation (92) may not be sufficient. In these cases, atomic vibrations may provide insight into origins of stress and material coefficients [22,38,65]. Also excluded from the analysis are noncentrosymmetric polyatomic lattices such as diamond and silicon that may incur inner displacements [54].

4.3 Harmonic and Anharmonic Interactions. Expanding the potential energy of Eq. (87) in a series about the reference state, let

$$\Phi = \Phi_0 + \sum_{i\neq j} \left.\frac{\partial \Phi}{\partial r^a_{\langle ij\rangle}}\right|_{\mathbf{r}=\mathbf{R}} q^a_{\langle ij\rangle} + \frac{1}{2!}\sum_{\substack{i\neq j\\ k\neq l}} \left.\frac{\partial^2 \Phi}{\partial r^a_{\langle ij\rangle}\,\partial r^b_{\langle kl\rangle}}\right|_{\mathbf{r}=\mathbf{R}} q^a_{\langle ij\rangle} q^b_{\langle kl\rangle} + \frac{1}{3!}\sum_{\substack{i\neq j\\ k\neq l\\ m\neq n}} \left.\frac{\partial^3 \Phi}{\partial r^a_{\langle ij\rangle}\,\partial r^b_{\langle kl\rangle}\,\partial r^c_{\langle mn\rangle}}\right|_{\mathbf{r}=\mathbf{R}} q^a_{\langle ij\rangle} q^b_{\langle kl\rangle} q^c_{\langle mn\rangle} + \cdots \tag{94}$$

where Φ_0 is the cohesive or ground state energy of the reference lattice, $\mathbf{q}_{\langle ij\rangle} = \mathbf{r}_{\langle ij\rangle} - \mathbf{R}_{\langle ij\rangle}$ is the relative displacement between atomic pairs, and the second term vanishes by Eqs. (86) and (88) since the reference configuration B_0 is explicitly chosen free of external and internal forces:

$$\left.\frac{\partial \Phi}{\partial r^a_{\langle ij\rangle}}\right|_{\mathbf{r}=\mathbf{R}} = 0 \tag{95}$$

Following the scheme first used in Eq. (90), repeated use of the summation symbol is omitted in Eq. (94). Hence, summation in the second term on the right side of Eq. (94) applies over two sets of repeated atomic labels, that in the third term over four sets, and that in the fourth term over six sets. The energy Ψ in Eq. (92) differs from the strain energy per reference volume Ψ_0 used in Sec. 3 by the constant $\Phi_0/\Omega_0 = \Psi - \Psi_0$, since continuum energy (31) vanishes in the reference state. Introducing the matrix notation

$$H^{ab}_{\langle ijkl\rangle} = \delta^{ac}\delta^{bd} \left.\frac{\partial^2 \Phi}{\partial r^c_{\langle ij\rangle}\,\partial r^d_{\langle kl\rangle}}\right|_{\mathbf{r}=\mathbf{R}}$$
$$H^{abc}_{\langle ijklmn\rangle} = \delta^{ad}\delta^{be}\delta^{cf} \left.\frac{\partial^3 \Phi}{\partial r^d_{\langle ij\rangle}\,\partial r^e_{\langle kl\rangle}\,\partial r^f_{\langle mn\rangle}}\right|_{\mathbf{r}=\mathbf{R}} \tag{96}$$

and noting that $\partial q^a_{\langle kl\rangle}/\partial r^b_{\langle kl\rangle} = \delta^a_{.b}$, the average spatial stress of Eqs. (90) and (93) becomes

$$\sigma^{ab} = \frac{1}{2\Omega}\sum_{\substack{i\neq j\\ k\neq l}} r^a_{\langle ij\rangle} H^{bc}_{\langle ijkl\rangle}\delta_{cd} q^d_{\langle kl\rangle} + \frac{1}{4\Omega}\sum_{\substack{i\neq j\\ k\neq l\\ m\neq n}} r^a_{\langle ij\rangle} H^{bce}_{\langle ijklmn\rangle}\delta_{cd} q^d_{\langle kl\rangle}\delta_{ef} q^f_{\langle mn\rangle} + \cdots \tag{97}$$

Since $\mathbf{r}_{\langle ij\rangle} = -\mathbf{r}_{\langle ji\rangle}$, the atomic stiffness matrix in the first of Eq. (96) exhibits the natural symmetries

$$H^{ab}_{\langle ijkl\rangle} = H^{ab}_{\langle jilk\rangle} = H^{ba}_{\langle klij\rangle} = -H^{ab}_{\langle jikl\rangle} = -H^{ab}_{\langle ijlk\rangle} = -H^{ba}_{\langle klji\rangle} \tag{98}$$

Similar symmetries can be deduced for $H^{abc}_{\langle ijklmn\rangle}$. Under a homogeneous deformation $\mathbf{q}_{\langle ij\rangle} = (\mathbf{F}-\mathbf{1})\mathbf{R}_{\langle ij\rangle}$,

$$P^{aA} = \frac{1}{2\Omega_0}\sum_{\substack{i\neq j\\ k\neq l}} H^{ab}_{\langle ijkl\rangle}\delta_{bc} q^c_{\langle kl\rangle} R^A_{\langle ij\rangle} + \frac{1}{4\Omega_0}\sum_{\substack{i\neq j\\ k\neq l\\ m\neq n}} H^{abc}_{\langle ijklmn\rangle}\delta_{bd} q^d_{\langle kl\rangle}\delta_{ce} q^e_{\langle mn\rangle} R^A_{\langle ij\rangle} + \cdots \tag{99}$$

In the harmonic approximation, products of order higher than 2 in atomic displacements $\mathbf{q}$ are dropped from Eq. (94), leading to

$$f^a_{\langle ij\rangle} = \sum_{k\neq l} H^{ab}_{\langle ijkl\rangle}\delta_{bc} q^c_{\langle kl\rangle}, \quad \sigma^{ab} = \frac{1}{2\Omega}\sum_{\substack{i\neq j\\ k\neq l}} r^a_{\langle ij\rangle} H^{bc}_{\langle ijkl\rangle}\delta_{cd} q^d_{\langle kl\rangle}$$
$$P^{aA} = \frac{1}{2\Omega_0}\sum_{\substack{i\neq j\\ k\neq l}} H^{ab}_{\langle ijkl\rangle}\delta_{bc} q^c_{\langle kl\rangle} R^A_{\langle ij\rangle} \tag{100}$$

A two-point elasticity tensor (i.e., tangent modulus) for homogeneous deformations can be found as

$$\mathrm{A}^{aAbB} = \frac{\partial P^{aA}}{\partial F_{bB}} = \frac{\partial^2 \Psi}{\partial F_{aA}\,\partial F_{bB}} = \frac{1}{2\Omega_0}\sum_{\substack{i\neq j\\ k\neq l}} \frac{\partial^2 \Phi}{\partial r^c_{\langle ij\rangle}\,\partial r^d_{\langle kl\rangle}}\frac{\partial r^c_{\langle ij\rangle}}{\partial F_{aA}}\frac{\partial r^d_{\langle kl\rangle}}{\partial F_{bB}} = \frac{1}{2\Omega_0}\sum_{\substack{i\neq j\\ k\neq l}} \frac{\partial^2 \Phi}{\partial r^c_{\langle ij\rangle}\,\partial r^d_{\langle kl\rangle}}\delta^{ac} R^A_{\langle ij\rangle}\delta^{bd} R^B_{\langle kl\rangle} \tag{101}$$

Defining the finite strain measure $E_{AB} = (F^a_{.A}\delta_{ab}F^b_{.B} - \delta_{AB})/2$ and noting that

$$\frac{\partial^2 \Psi}{\partial E_{AB}\,\partial E_{CD}} = \left(\mathrm{A}^{aBcD} - \frac{\partial \Psi}{\partial E_{BD}}\delta^{ac}\right) F^{-1A}_{.a} F^{-1C}_{.c} \tag{102}$$

the average second-order elastic constants in the reference state are defined from atomic quantities as

$$\mathbb{C}^{ABCD} = \delta^A_{.a}\delta^C_{.c}\mathrm{A}^{aBcD}\big|_{\mathbf{F}=\mathbf{1}} = \frac{1}{2\Omega_0}\sum_{\substack{i\neq j\\ k\neq l}} H^{ab}_{\langle ijkl\rangle}\delta^A_{.a} R^B_{\langle ij\rangle}\delta^C_{.b} R^D_{\langle kl\rangle} \tag{103}$$

and clearly depend only on the harmonic part of the potential. Similarly, for third-order coefficients

$$\mathrm{A}^{aAbBcC} = \frac{\partial^2 P^{aA}}{\partial F_{bB}\,\partial F_{cC}} = \frac{\partial^3 \Psi}{\partial F_{aA}\,\partial F_{bB}\,\partial F_{cC}} = \frac{1}{2\Omega_0}\sum_{\substack{i\neq j\\ k\neq l\\ m\neq n}} \frac{\partial^3 \Phi}{\partial r^d_{\langle ij\rangle}\,\partial r^e_{\langle kl\rangle}\,\partial r^f_{\langle mn\rangle}}\delta^{ad} R^A_{\langle ij\rangle}\delta^{be} R^B_{\langle kl\rangle}\delta^{cf} R^C_{\langle mn\rangle} \tag{104}$$

Differentiating Eq. (102) with respect to $\mathbf{E}$ gives

$$\frac{\partial^3 \Psi}{\partial E_{AE}\,\partial E_{BD}\,\partial E_{CG}} = \left(\mathrm{A}^{aAbBcC} - \frac{\partial^2 \Psi}{\partial E_{AB}\,\partial E_{CF}}\delta^{ab}F^c_{.F} - \frac{\partial^2 \Psi}{\partial E_{AC}\,\partial E_{BF}}\delta^{ac}F^b_{.F} - \frac{\partial^2 \Psi}{\partial E_{AF}\,\partial E_{BC}}\delta^{bc}F^a_{.F}\right) \times F^{-1E}_{.a} F^{-1D}_{.b} F^{-1G}_{.c} \tag{105}$$

Third-order elastic constants at the reference state are then

$$\mathbb{C}^{ABCDEF} = \mathrm{A}^{aAbCcE}|_{\mathbf{F}=\mathbf{1}}\delta^B_{.a}\delta^D_{.b}\delta^F_{.c} - \mathbb{C}^{ACEF}\delta^{BD} - \mathbb{C}^{AECD}\delta^{BF} - \mathbb{C}^{ABCE}\delta^{DF}$$

$$= \frac{1}{2\Omega_0}\sum_{\substack{i\neq j\\ k\neq l\\ m\neq n}} H^{abc}_{\langle ijklmn\rangle}R^A_{\langle ij\rangle}R^C_{\langle kl\rangle}R^E_{\langle mn\rangle}\delta^B_{.a}\delta^D_{.b}\delta^F_{.c} - \frac{1}{2\Omega_0}\sum_{\substack{i\neq j\\ k\neq l}} H^{ab}_{\langle ijkl\rangle}\delta^A_{.a}R^C_{\langle ij\rangle}\delta^E_{.b}R^F_{\langle kl\rangle}\delta^{BD} - \frac{1}{2\Omega_0}\sum_{\substack{i\neq j\\ k\neq l}} H^{ab}_{\langle ijkl\rangle}\delta^A_{.a}R^E_{\langle ij\rangle}\delta^C_{.b}R^D_{\langle kl\rangle}\delta^{BF} - \frac{1}{2\Omega_0}\sum_{\substack{i\neq j\\ k\neq l}} H^{ab}_{\langle ijkl\rangle}\delta^A_{.a}R^B_{\langle ij\rangle}\delta^C_{.b}R^E_{\langle kl\rangle}\delta^{DF} \tag{106}$$

Relation (106) indicates that third-order elastic constants depend in part on anharmonic terms in the potential [48,66]. Derivations (99), (101), (103), (104), and (106) rely on uniformity of the atomistic deformation, such that the relationship between current position vector $\mathbf{r}$ and reference position vector $\mathbf{R}$ is linear in the mapping $\mathbf{F}$. In this atomistic context, $\mathbf{F}$ is regarded as a linear transformation for the primitive Bravais lattice vectors (e.g., akin to $\mathbf{F}^{\mathbf{L}}$ in Eq. (12)), and though it acts uniformly over atoms in an individual element of reference volume Ω_0, $\mathbf{F}$ or $\mathbf{F}^{\mathbf{L}}$ need not be the gradient of any macroscopic vector field spanning neighboring volume elements [51]. In contrast, determination of deformation gradient measures for individual atoms of a body undergoing heterogeneous deformation is more involved [67]. Expansion (94), while generic in the sense that many types of interactions (e.g., pairwise and multibody, and central and noncentral forces) are admitted, may be cumbersome for computation of elastic constants for specific potentials not expressed explicitly in terms of interatomic separation vectors. For example, expressions for second- and third-order elastic constants for cubic crystals obtained from the embedded atom method are available [68] in terms of derivatives with respect to scalar interatomic distances. However, these expressions [68] for second- and third-order elastic constants analogously contain derivatives of up to orders 2 and 3, respectively, of the potential functions.

4.4 Net Residual Deformation in a Self-Equilibrated Lattice. Now consider self-equilibrated configuration $\overline{B}$ of Fig. 1. Slip may have occurred in achieving this configuration from the reference state, but atoms occupy perfect lattice sites apart from the effects of any defects remaining within the element that either (i) are also present in the reference configuration B_0 or (ii) are generated during the course of plastic deformation. Not considered here is the (former) class of defects present in B_0. Although positions of specific atoms differ in configurations B_0 and $\tilde{B}$ as a result of translations by Burgers vectors of dislocations that have passed through the volume element, coordinates $\mathbf{R}_{\langle i\rangle}$ can still be used to identify positions of atoms occupying perfect lattice sites in $\tilde{B}$ [51]. The volume element may either be treated as an isolated ensemble of atoms with free boundaries or as part of an infinite medium with a periodic defect distribution. The former case is more consistent with the fundamental definition of the isolated unloaded configuration [26] given in Sec. 2, while the latter case—which implicitly includes the effects of image forces of defects in neighboring volume elements—may be more practical from the standpoint of lattice statics calculations with periodic boundary conditions [69]. Previous definitions for achieving slipped configuration $\tilde{B}$ discussed in Sec. 2.1 still apply here, but dislocation fluxes contributing to the plastic deformation are now interpreted in terms of velocities of atoms comprising each line defect rather than as continuum quantities. External forces vanish by definition in $\overline{B}$, as do dynamics (i.e., atomic velocities and accelerations), so lattice statics relation (86) applies for a self-equilibrated lattice. However, because of the presence of defects, the stable total energy of the ensemble $\mathcal{L}$ of atoms in $\overline{B}$ is a local minimum [47,69] as opposed to the global minimum corresponding to perfect lattice in B_0. This implies that some atoms occupy metastable positions; some interatomic (i.e., internal) forces do not vanish within the element in $\overline{B}$ as they do in B_0 according to Eq. (95); and the potential energy in $\overline{B}$ exceeds Φ_0. Existence of a metastable state of local minimum energy results from a lack of strict convexity of the total potential energy.

The position of atom i in configuration $\overline{B}$ is denoted by $\overline{\mathbf{r}}_{\langle i\rangle}$. Because $\overline{B}$ is self-equilibrated, average static atomic stress measures vanished by definition:

$$\overline{\sigma}^{ab} = \frac{1}{2\overline{\Omega}}\sum_{i\neq j}\overline{r}^a_{\langle ij\rangle}\delta^{bc}\frac{\partial\Phi}{\partial\overline{r}^c_{\langle ij\rangle}} = 0, \quad \overline{P}^{aA} = \frac{1}{2\Omega_0}\sum_{i\neq j}\delta^{ab}\frac{\partial\Phi}{\partial\overline{r}^b_{\langle ij\rangle}}R^A_{\langle ij\rangle} = 0 \tag{107}$$

with $\overline{\Omega}=\overline{J}\Omega_0$ the system volume in $\overline{B}$, Φ the potential energy of Eq. (87), and $\overline{\mathbf{r}}_{\langle ij\rangle}=\overline{\mathbf{r}}_{\langle j\rangle}-\overline{\mathbf{r}}_{\langle i\rangle}$. Because atomic coordinates are not mapped homogeneously from their positions in B_0 to their positions in $\overline{B}$, the average first Piola–Kirchhoff stress measure in the second of Eq. (107) does not follow from a linear transformation such as used in the chain rule in Eq. (92); it is instead introduced as a fundamental definition. Equation (107) contains discrete analogs of continuum relations (23) and (29). Here as in Eq. (94), the potential energy is expanded in a series about a perfect reference configuration:

$$\Phi = \Phi_0 + \frac{1}{2}\sum_{\substack{i\neq j\\ k\neq l}} H^{ab}_{\langle ijkl\rangle}\delta_{ac}\overline{q}^c_{\langle ij\rangle}\delta_{bd}\overline{q}^d_{\langle kl\rangle} + \frac{1}{6}\sum_{\substack{i\neq j\\ k\neq l\\ m\neq n}} H^{abc}_{\langle ijklmn\rangle}\delta_{ad}\overline{q}^d_{\langle ij\rangle}\delta_{be}\overline{q}^e_{\langle kl\rangle}\delta_{cf}\overline{q}^f_{\langle mn\rangle} + \ldots \tag{108}$$

with $\overline{\mathbf{q}}_{\langle ij\rangle}=\overline{\mathbf{r}}_{\langle ij\rangle}-\mathbf{R}_{\langle ij\rangle}$ the displacement difference between two atoms in the defective lattice, and where Eqs. (95) and (96) have been used to define atomic stiffness coefficients in Eq. (108). Substituting Eq. (108) into the first of Eq. (107) and multiplying through by $\overline{J}$, the null average atomic stress relation becomes

$$0 = \overline{J}\overline{\sigma}^{fa} = \frac{1}{2\Omega_0}\sum_{\substack{i\neq j\\ k\neq l}}\overline{r}^f_{\langle ij\rangle}H^{ab}_{\langle ijkl\rangle}\delta_{bc}\overline{q}^c_{\langle kl\rangle} + \frac{1}{4\Omega_0}\sum_{\substack{i\neq j\\ k\neq l\\ m\neq n}}\overline{r}^f_{\langle ij\rangle}H^{abc}_{\langle ijklmn\rangle}\delta_{bd}\overline{q}^d_{\langle kl\rangle}\delta_{ce}\overline{q}^e_{\langle mn\rangle} + \ldots \tag{109}$$

Just as in Eqs. (36)–(40), vanishing of the average symmetric stress measured in the reference configuration leads by definition to six equations for six unknown components of the symmetric deformation map $\mathbf{F}^{\mathbf{I}}$. Identifying harmonic terms in the atomic definition of the average stress with linear terms in the continuum elastic definition of the average stress:

$$\underbrace{\frac{1}{V}\int_V \mathbb{C}^{ABCD}u_{C,D}dV}_{\text{continuum elasticity}} \Leftrightarrow \underbrace{\frac{1}{2\Omega_0}\delta^A_{.f}\delta^B_{.a}\sum_{\substack{i\neq j\\ k\neq l}} \overline{r}^f_{\langle ij\rangle}H^{ab}_{\langle ijkl\rangle}\delta_{bc}\overline{q}^c_{\langle kl\rangle}}_{\text{discrete lattice statics}} \tag{110}$$

the following definition emerges:

$$\begin{aligned}\mathbb{C}^{ABCD}(F^I_{CD}-\delta_{CD}) &= \frac{1}{2\Omega_0}\delta^A_{.f}\delta^B_{.a}\sum_{\substack{i\neq j\\ k\neq l}} \overline{r}^f_{\langle ij\rangle}H^{ab}_{\langle ijkl\rangle}\delta_{bc}\overline{q}^c_{\langle kl\rangle}\\ &= -\frac{1}{4\Omega_0}\delta^A_{.f}\delta^B_{.a}\sum_{\substack{i\neq j\\ k\neq l\\ m\neq n}} \overline{r}^f_{\langle ij\rangle}H^{abc}_{\langle ijklmn\rangle}\delta_{bd}\overline{q}^d_{\langle kl\rangle}\delta_{ce}\overline{q}^e_{\langle mn\rangle}\\ &\quad -\ldots\end{aligned} \tag{111}$$

with the second equality following directly from Eq. (109). Assuming that the reference stiffness of the perfect lattice $\mathbb{C}^{ABCD}$ is positive definite,

$$F^I_{CD}=\delta_{CD} - \frac{1}{\Omega_0}\mathrm{S}_{CDAB}\left[(\delta^A_{.f}\delta^B_{.a}/4)\sum_{\substack{i\neq j\\ k\neq l\\ m\neq n}} \overline{r}^f_{\langle ij\rangle}H^{abc}_{\langle ijklmn\rangle}\delta_{bd}\overline{q}^d_{\langle kl\rangle}\delta_{ce}\overline{q}^e_{\langle mn\rangle}+\ \ldots\right] \tag{112}$$

where the compliance S_{CDAB} satisfies Eq. (41) and can be found from inverting the second-order reference moduli, the latter either computed using Eq. (103) and the chain rule or computed from expressions available for particular potentials [68]. The series in brackets on the right of Eq. (112) accounts for anharmonic interactions, and includes terms of order 2 and higher in relative atomic displacements $\overline{q}^a_{\langle ij\rangle}$ in the locally deformed, yet self-equilibrated, defective lattice. For harmonic lattice statics, in which case $H^{abc}_{\langle ijklmn\rangle}=0$ and/or quadratic and higher-order terms in $\overline{q}^a_{\langle ij\rangle}$ are dropped, the bracketed series degenerates to zero and $F^I_{CD}=\delta_{CD}$, analogously to linear continuum description (38). The definition for F^I_{CD} implied by the first of Eq. (111), while not unique, is motivated by the corresponding continuum definition $F^I_{CD}=V^{-1}\int x_{(C,D)}dV=V^{-1}\mathrm{S}_{CDAB}\mathbb{C}^{ABEF}\int x_{(E,F)}dV$ in Eqs. (35) and (40). Following Sec. 3.6, the first-order accurate residual volume change is $\overline{J}=\overline{\Omega}/\Omega_0\approx\det(F^I_{CD})\approx F^{IC}_{.C}-\delta^C_{.C}+1$, where continuum and discrete measures of reference and intermediate volumes are related, respectively, by $\Omega_0=V$ and $\overline{\Omega}=V+\Delta V$. Calculation of this volume change does not require identification of a bounding surface delineating the volume occupied by the atoms in configuration $\overline{B}$, i.e., the atoms can occupy an arbitrary shape so long as their interaction forces self-equilibrate. If such a surface can be identified in a lattice statics calculation, for example, an ensemble of atoms in a defective state contained within a hexahedral bounding box, it should be possible to compute $\overline{\Omega}$ trivially (i.e., $\overline{\Omega}$ is then the volume of the box) and then compare the results with the predictions of Eq. (112), so long as the average static virial stress vanishes over the defective ensemble of atoms. An apparent advantage of the atomistic approach over the continuum approach of Sec. 3 is that effects of defect cores are accurately incorporated in the former, presuming that the atomic potential is sufficiently robust to address defect core structures. An apparent disadvantage is that solutions to Eq. (112) must be computed numerically, while the continuum elastic approach [8,43,44] provides convenient analytical formulas for volume changes such as Eqs. (61) and (74).

5 Conclusions

A three-term decomposition for finite multiplicative elastoplasticity of a volume element of a crystalline solid has been described. Isochoric plastic deformation arises from displacement discontinuities such as those resulting from cumulative slip of dislocations. Lattice deformation consists of two parts: (i) that arising from recoverable straining due to external loading and rotation of the lattice vectors and (ii) that arising from residual elasticity present when the volume element is self-equilibrated. Local displacement gradient fields within the element contributing to the latter (i.e., contributing to the average residual elastic strain) are conjugate to local elastic stress fields associated with lattice defects, for example, eigenstresses of dislocation and disclination lines and loops. Two methods are used to quantify the average residual elastic strain. The first treats the body as a nonlinear hyperelastic solid with spatially constant moduli. In this case, the strain energy is expanded in a series of up to order 3 in displacement gradients. An integral equation for the average residual elastic strain is obtained from the equilibrium conditions requiring the average stress to vanish. It follows that this average residual strain vanishes identically only when terms of order 3 are discarded, i.e., when the body is treated as linear elastic. The second method follows from treating the body as a set of discrete atoms in the context of molecular or lattice statics. The potential energy is expanded in a series about a reference state, wherein interatomic forces and average atomic stresses (i.e., average static virial stress components) vanish. When the series contains only terms of up to order 2 in relative interatomic displacements (i.e., harmonic lattice statics), average dimensional changes of the lattice consisting of an ensemble of atoms in a defective arrangement are negligible according to the definitions used here. On the other hand, when anharmonic terms are retained in the series expansion of the potential energy, average dimensional changes do not always vanish identically. Particular attention has been given to average volume changes resulting from strain energy of line defects in an externally unstressed body, and examples for dislocation and disclination lines and loops have been tabulated and compared with experimental data for copper. Theoretical predictions and experimental measurements for volumetric expansion resulting from dislocation and disclination lines or loops agree within about a factor of 2. Because average residual elastic deformation results from nonlinear elastic effects, i.e., products of displacement gradients of orders 2 and higher in the continuum treatment, or from anharmonic effects, i.e., nonlinear force-displacement relations in the atomistic treatment, the contribution of average residual elastic deformation to the total deformation gradient will generally be small in conventional engineering applications wherein defect densities remain small to moderate, as observed experimentally for volume changes in metallic crystals deformed quasistatically to macroscopic shear or compressive strains on the order of unity. However, for situations in which defect densities are extremely large, such as severe plastic deformation processes or shock loading, the theory suggests that the net contribution of residual elasticity from defects, especially volume changes, to the overall deformation gradient could affect measured properties such as the apparent bulk modulus and its pressure derivatives.

References

[1] Orowan, E., 1940, "Problems of Plastic Gliding," Proc. Phys. Soc. London, **52**, pp. 8–22.

[2] Mura, T., 1968, "Continuum Theory of Dislocations and Plasticity," *Mechanics of Generalized Continua*, E. Kroner, ed., Springer-Verlag, New York, pp. 269–278.

[3] Bilby, B. A., Gardner, L. R. T., and Stroh, A. N., 1957, "Continuous Distributions of Dislocations and the Theory of Plasticity," Proceedings of the Ninth International Congress of Applied Mechanics, Bruxelles, Vol. 8, pp. 35–44.

[4] Teodosiu, C., 1970, "A Dynamic Theory of Dislocations and Its Applications to the Theory of the Elastic-Plastic Continuum," *Fundamental Aspects of Dislocation Theory*, J. A. Simmons, R. De Wit, and R. Bullough, eds., U.S. Natl. Bur. Stand. Spec. Publ. No. 317, Washington, DC, Vol. II, pp. 837–876.

[5] Rice, J. R., 1971, "Inelastic Constitutive Relations for Solids: An Internal

Variable Theory and Its Application to Metal Plasticity," J. Mech. Phys. Solids, **19**, pp. 433–455.
[6] De Wit, R., 1973, "Theory of Disclinations II, III, IV," J. Res. Nat. Bureau Standards A Phys. Chem., **77**, pp. 49–100, 359–368, 607–658.
[7] Mura, T., 1982, *Micromechanics of Defects in Solids*, Martinus Nijhoff, Dordrecht.
[8] Zener, C., 1942, "Theory of Lattice Expansion Introduced by Cold Work," Trans. Am. Inst. Min. Metall. Engrs., **147**, pp. 361–368.
[9] Schmid, E., and Boas, I. W., 1950, *Plasticity of Crystals*, Chapman and Hall, London.
[10] Holder, J., and Granato, A. V., 1969, "Thermodynamic Properties of Solids Containing Defects," Phys. Rev., **182**, pp. 729–741.
[11] Wright, T. W., 1982, "Stored Energy and Plastic Volume Change," Mech. Mater., **1**, pp. 185–187.
[12] Taheri, M., Weiland, H., and Rollett, A., 2006, "A Method of Measuring Stored Energy Macroscopically Using Statistically Stored Dislocations in Commercial Purity Aluminum," Metall. Mater. Trans. A, **37**, pp. 19–25.
[13] Rosakis, P., Rosakis, A. J., Ravichandran, G., and Hodowany, J., 2000, "A Thermodynamic Internal Variable Model for the Partition of Plastic Work Into Heat and Stored Energy in Metals," J. Mech. Phys. Solids, **48**, pp. 581–607.
[14] Rohatgi, A., and Vecchio, K. S., 2002, "The Variation of Dislocation Density as a Function of the Stacking Fault Energy in Shock-Deformed FCC Materials," Mater. Sci. Eng., A, **328**, pp. 256–266.
[15] Clayton, J. D., 2009, "A Continuum Description of Nonlinear Elasticity, Slip and Twinning, With Application to Sapphire," Proc. R. Soc. London, Ser. A, **465**, pp. 307–334.
[16] Clayton, J. D., Bammann, D. J., and McDowell, D. L., 2005, "A Geometric Framework for the Kinematics of Crystals With Defects," Philos. Mag., **85**, pp. 3983–4010.
[17] Clayton, J. D., McDowell, D. L., and Bammann, D. J., 2006, "Modeling Dislocations and Disclinations With Finite Micropolar Elastoplasticity," Int. J. Plast., **22**, pp. 210–256.
[18] Li, J. C. M., and Gilman, J. T., 1970, "Disclination Loops in Polymers," J. Appl. Phys., **41**, pp. 4248–4256.
[19] Eshelby, J. D., 1954, "Distortion of a Crystal Caused by Point Imperfections," J. Appl. Phys., **25**, pp. 255–261.
[20] Eshelby, J. D., 1956, "The Continuum Theory of Lattice Defects," *Solid State Physics 3*, F. Seitz and D. Turnbull, eds., Academic, New York, pp. 79–144.
[21] Hirth, J. P., and Lothe, J., 1982, *Theory of Dislocations*, Krieger, Malabar, FL.
[22] Born, M., and Huang, K., 1954, *Dynamical Theory of Crystal Lattices*, Oxford University Press, Oxford.
[23] Ericksen, J. L., 1984, "The Cauchy and Born Hypothesis for Crystals," *Phase Transformations and Material Instabilities in Solids*, M. E. Gurtin, ed., Academic, New York, pp. 61–78.
[24] Kroner, E., 1960, "Allgemeine kontinuumsthoerie der versetzungen und eigenspannungen," Arch. Ration. Mech. Anal., **4**, pp. 273–334.
[25] Lee, E. H., 1969, "Elastic-Plastic Deformation at Finite Strains," ASME J. Appl. Mech., **36**, pp. 1–6.
[26] Eckart, C., 1948, "The Thermodynamics of Irreversible Processes IV. The Theory of Elasticity and Anelasticity," Phys. Rev., **73**, pp. 373–382.
[27] Kroner, E., and Seeger, A., 1959, "Nicht-Lineare Elastizitatstheorie der Versetzungen und Eigenspannungen," Arch. Ration. Mech. Anal., **3**, pp. 97–119.
[28] Willis, J. R., 1967, "Second-Order Effects of Dislocations in Anisotropic Crystals," Int. J. Eng. Sci., **5**, pp. 171–190.
[29] Teodosiu, C., 1982, *Elastic Models of Crystal Defects*, Springer-Verlag, Berlin.
[30] Nye, J. F., 1953, "Some Geometrical Relations in Dislocated Crystals," Acta Metall., **1**, pp. 153–162.
[31] Kondo, K., 1964, "On the Analytical and Physical Foundations of the Theory of Dislocations and Yielding by the Differential Geometry of Continua," Int. J. Eng. Sci., **2**, pp. 219–251.
[32] Steinmann, P., 1996, "Views on Multiplicative Elastoplasticity and the Continuum Theory of Dislocations," Int. J. Eng. Sci., **34**, pp. 1717–1735.
[33] Shizawa, K., and Zbib, H., 1999, "A Thermodynamical Theory of Plastic Spin and Internal Stress With Dislocation Density Tensor," ASME J. Eng. Mater. Technol., **121**, pp. 247–253.
[34] Bammann, D. J., 2001, "A Model of Crystal Plasticity Containing a Natural Length Scale," Mater. Sci. Eng., A, **309–310**, pp. 406–410.
[35] Regueiro, R. A., Bammann, D. J., Marin, E. B., and Garikipati, K., 2002, "A Nonlocal Phenomenological Anisotropic Finite Deformation Plasticity Model Accounting for Dislocation Defects," ASME J. Eng. Mater. Technol., **124**, pp. 380–387.
[36] Clayton, J. D., Bammann, D. J., and McDowell, D. L., 2004, "A Multiscale Gradient Theory for Elastoviscoplasticity of Single Crystals," Int. J. Eng. Sci., **42**, pp. 427–457.
[37] Clayton, J. D., Chung, P. W., Grinfeld, M. A., and Nothwang, W. D., 2008, "Kinematics, Electromechanics, and Kinetics of Dielectric and Piezoelectric Crystals With Lattice Defects," Int. J. Eng. Sci., **46**, pp. 10–30.
[38] Huang, K., 1950, "On the Atomic Theory of Elasticity," Proc. R. Soc. London, Ser. A, **203**, pp. 178–194.
[39] Lardner, R. W., 1969, "Dislocation Dynamics and the Theory of the Plasticity of Single Crystals," Z. Angew. Math. Phys., **20**, pp. 514–529.
[40] Kratochvil, J., 1972, "Finite Strain Theory of Inelastic Behavior of Crystalline Solids," *Foundations of Plasticity*, A. Sawczuk, ed., Noordhoff, Leyden, pp. 401–415.
[41] Hartley, C. S., 2003, "A Method for Linking Thermally Activated Dislocation Mechanisms of Yielding With Continuum Plasticity Theory," Philos. Mag., **83**, pp. 3783–3808.
[42] Clayton, J. D., and McDowell, D. L., 2003, "A Multiscale Multiplicative Decomposition for Elastoplasticity of Polycrystals," Int. J. Plast., **19**, pp. 1401–1444.
[43] Seeger, A., and Haasen, P., 1958, "Density Changes of Crystals Containing Dislocations," Philos. Mag., **3**, pp. 470–475.
[44] Toupin, R. A., and Rivlin, R. S., 1960, "Dimensional Changes in Crystals Caused by Dislocations," J. Math. Phys., **1**, pp. 8–15.
[45] Glarebrough, L. M., Hargreaves, M. E., and West, G. W., 1957, "The Density of Dislocations in Compressed Copper," Acta Metall., **5**, pp. 738–740.
[46] Zhou, M., 2003, "A New Look at the Atomic Level Virial Stress: On Continuum-Molecular System Equivalence," Proc. R. Soc. London, Ser. A, **459**, pp. 2347–2392.
[47] Gallego, R., and Ortiz, M., 1993, "A Harmonic/Anharmonic Energy Partition Method for Lattice Statics Computations," Modell. Simul. Mater. Sci. Eng., **1**, pp. 417–436.
[48] Maugin, G. A., 1999, *Nonlinear Waves in Elastic Crystals*, Oxford University Press, New York.
[49] Yavari, A., Ortiz, M., and Bhattacharya, K., 2007, "A Theory of Anharmonic Lattice Statics for Analysis of Defective Crystals," J. Elast., **86**, pp. 41–83.
[50] Horstemeyer, M. F., and Baskes, M. I., 1999, "Atomic Finite Deformation Simulations: A Discussion on Length Scale Effects in Relation to Mechanical Stress," ASME J. Eng. Mater. Technol., **121**, pp. 114–119.
[51] Clayton, J. D., and Chung, P. W., 2006, "An Atomistic-to-Continuum Framework for Nonlinear Crystal Mechanics Based on Asymptotic Homogenization," J. Mech. Phys. Solids, **54**, pp. 1604–1639.
[52] Zbib, H. M., Rubia, T. D. L., and Bulatov, V., 2002, "A Multiscale Model of Plasticity Based on Discrete Dislocation Dynamics," ASME J. Eng. Mater. Technol., **124**, pp. 78–87.
[53] Asaro, R. J., 1983, "Crystal Plasticity," ASME J. Appl. Mech., **50**, pp. 921–934.
[54] Tadmor, E. B., Smith, G. S., Bernstein, N., and Kaxiras, E., 1999, "Mixed Finite Element and Atomistic Formulation for Complex Crystals," Phys. Rev. B, **59**, pp. 235–245.
[55] Hill, R., 1972, "On Constitutive Macro-Variables for Heterogeneous Solids at Finite Strain," Proc. R. Soc. London, Ser. A, **326**, pp. 131–147.
[56] Clayton, J. D., and McDowell, D. L., 2004, "Homogenized Finite Elastoplasticity and Damage: Theory and Computations," Mech. Mater., **36**, pp. 799–824.
[57] Hull, D., and Bacon, D. J., 1984, *Introduction to Dislocations*, 3rd ed., Butterworth-Heinemann, Oxford.
[58] Thurston, R. N., 1974, "Waves in Solids," *Handbuch der Physik*, Vol. VIa/4, C. Truesdell, ed., Springer-Verlag, Berlin, pp. 109–308.
[59] Owen, D. J. R., and Mura, T., 1967, "Dislocation Configurations in Cylindrical Coordinates," J. Appl. Phys., **38**, pp. 2818–2825.
[60] Huang, W., and Mura, T., 1970, "Elastic Fields and Energies of a Circular Edge Disclination and a Straight Screw Disclination," J. Appl. Phys., **41**, pp. 5175–5179.
[61] Liu, G. C. T., and Li, J. C. M., 1971, "Strain Energies of Disclination Loops," J. Appl. Phys., **42**, pp. 3313–3315.
[62] Kuo, H. H., and Mura, T., 1972, "Elastic Field and Strain Energy of a Circular Wedge Disclination," J. Appl. Phys., **43**, pp. 1454–1457.
[63] Hughes, D. A., Hansen, N., and Bammann, D. J., 2003, "Geometrically Necessary Boundaries, Incidental Dislocation Boundaries, and Geometrically Necessary Dislocations," Scr. Mater., **48**, pp. 147–153.
[64] Zimmerman, J. A., Webb, E. B., III, Hoyt, J. J., Jones, R. E., Klein, P. A., and Bammann, D. J., 2004, "Calculation of Stress in Atomistic Simulation," Modell. Simul. Mater. Sci. Eng., **12**, pp. S319–S332.
[65] Mindlin, R. D., 1972, "Elasticity, Piezoelectricity, and Crystal Lattice Dynamics," J. Elast., **2**, pp. 217–282.
[66] Thurston, R. N., and Brugger, K., 1964, "Third-Order Elastic Constants and the Velocity of Small Amplitude Elastic Waves in Homogeneously Stressed Media," Phys. Rev., **133**, pp. A1604–A1610.
[67] Zimmerman, J. A., Bammann, D. J., and Gao, H., 2009, "Deformation Gradients for Continuum Mechanical Analysis of Atomistic Simulations," Int. J. Solids Struct., **46**, pp. 238–253.
[68] Chantasiriwan, S., and Milstein, F., 1996, "Higher-Order Elasticity of Cubic Metals in the Embedded-Atom Method," Phys. Rev. B, **53**, pp. 14080–14088.
[69] Chung, P. W., and Clayton, J. D., 2007, "Multiscale Modeling of Point and Line Defects in Cubic Lattices," Int. J. Multiscale Comp. Eng., **5**, pp. 203–226.

NO. OF
COPIES ORGANIZATION

1 (PDF only) DEFENSE TECHNICAL INFORMATION CTR
DTIC OCA
8725 JOHN J KINGMAN RD
STE 0944
FORT BELVOIR VA 22060-6218

1 DIRECTOR
US ARMY RESEARCH LAB
IMNE ALC HRR
2800 POWDER MILL RD
ADELPHI MD 20783-1197

1 DIRECTOR
US ARMY RESEARCH LAB
RDRL CIM L
2800 POWDER MILL RD
ADELPHI MD 20783-1197

1 DIRECTOR
US ARMY RESEARCH LAB
RDRL CIM P
2800 POWDER MILL RD
ADELPHI MD 20783-1197

ABERDEEN PROVING GROUND

1 DIR USARL
RDRL CIM G (BLDG 4600)

NO. OF COPIES ORGANIZATION

1 DIRECTOR
US ARMY RESEARCH LAB
RDRL CI
R NAMBURU
2800 POWDER MILL RD
ADELPHI MD 20783-1197

ABERDEEN PROVING GROUND

45 DIR USARL
RDRL CIH C
P CHUNG
D GROVE
J KNAP
RDRL SL
R COATES
RDRL WM
B FORCH
S KARNA
J MCCAULEY
T WRIGHT
RDRL WMS
T JONES
RDRL WMM A
J ANDZELM
W NOTHWANG
RDRL WMM D
B CHEESEMAN
G GAZONAS
RDRL WMT A
R DONEY
S SCHOENFELD
RDRL WMT C
T BJERKE
T FARRAND
M FERMEN-COKER
S SEGLETES
B SCHUSTER
A TANK
W WALTERS
C WILLIAMS
RDR WMT D
S BILYK
D CASEM
J CLAYTON (10 CPS)
D DANDEKAR
N GNIAZDOWSKI
M GREENFIELD
Y HUANG
R KRAFT
B LOVE

NO. OF COPIES ORGANIZATION

M RAFTENBERG
E RAPACKI
M SCHEIDLER
T WEERASOORIYA

INTENTIONALLY LEFT BLANK.